Advanced State Transition Matrices Computation Algorithms

Trabajo Fin de Máster

Máster Universitario en Ingeniería Aeronáutica

Escuela Técnica Superior de Ingeniería

Aeronáutica y del Espacio

Universidad Politécnica de Madrid

Autor: Rodrigo Fernández Matilla

Tutor profesional: Víctor Manuel Moreno Villa

Tutor académico: Manuel Pérez Cortés

Septiembre 2022

Contents

Nomenclature

Physical constants

γ Coeficiente de dilatación adiabática de un gas $[-]$

T_C Temperatura del punto triple $[K]$

$\boldsymbol{\Lambda}$ Matriz de autovalores de un sistema de ecuaciones diferenciales

$\boldsymbol{\lambda}_i$ Autovalor i-ésimo de la matriz del sistema

$\boldsymbol{A}$ Matriz del sistema de una ecuación diferencial

$\boldsymbol{F}(\boldsymbol{U})$ Vector de flujos de una ecuación diferencial

$\boldsymbol{I}$ Matriz identidad

$\boldsymbol{K}^{(i)}$ Autovector i-ésimo de la matriz del sistema

$\boldsymbol{n}$ Vector normal exterior a una superficie

$\boldsymbol{R}$ Vector de términos fuente de una ecuación diferencial

$\boldsymbol{U}$ Vector de variables dependientes de un sistema de ecuaciones diferenciales

$\boldsymbol{U}$ Vector de variables dependientes de una ecuación diferencial

$\boldsymbol{W}$ Vector de variables dependientes canónicas de un sistema de ecuaciones diferenciales

$\mathbb{I}$ Unidad imaginaria

$\mathcal{L}(\boldsymbol{U})$ Operador diferencial espacial de una ecuación diferencial en derivadas parciales

Ω Volumen geométrico

$\partial\Omega$ Frontera del volumen Ω

ϕ Superficie característica de una ecuación diferencial en derivadas parciales

Σ Superficie geométrica

$d\gamma$, $d\sigma$, $d\omega$ Diferenciales de arco, superficie y volumen

s Parámetro de longitud de arco

Cartesian coordinates

$\bar{u}_i^n$ Solución exacta de un esquema numérico

$\boldsymbol{F}_{i+1/2}$ Flujos numéricos en el extremo superior del volumen finito i-ésimo

$\boldsymbol{Q}$ Vector de parámetros del método de Roe

$\boldsymbol{U}_{i+1/2}$ Solución computada en el extremo superior del volumen finito i-ésimo

Δx, Δt Pasos espacial y temporal

ϵ_T Error de truncamiento de un esquema numérico

λ_j Longitud de onda del armónico j-ésimo

ω Relación de dispersión numérica

Ω_i Volumen de control i-ésimo

ϕ_j Fase del armónico j-ésimo

σ Número CFL

$\tilde{\boldsymbol{A}}$ Matriz promediada del sistema

$\tilde{\lambda}_i$ Autovalor i-ésimo de la matriz promediada del sistema

$\tilde{\omega}$ Relación de dispersión

$\tilde{K}^{(i)}$ Autovector i-ésimo de la matriz promediada del sistema

$\tilde{u}_i^n$ Solución exacta de un modelo matemático

G_j Factor de amplificación o ganancia del armónico j-ésimo

I_i Centroide del volumen finito i-ésimo

k_j Número de onda del armónico j-ésimo

$N(\bullet)$ Esquema numérico

S Velocidad de propagación de una discontinuidad

S_{max}^n Velocidad máxima de propagación de información en un problema de evolución discretizado

u_i^n Solución computada de un esquema numérico

V_j^n Amplitud del armónico j-ésimo en el instante n-ésimo

$x_{i+1/2}$ Extremo superior del volumen finito i-ésimo

Characteristic numbers

Fr Número de Froude $\hspace{6cm} Fr = \dfrac{U_c}{\sqrt{g_0 L_c}}$

Nu Número de Nusselt $\hspace{6cm} Nu = \dfrac{h_c L_c}{k}$

Pr Número de Prandtl $\hspace{6.5cm} Pr = \dfrac{\nu}{\alpha}$

Re Número de Reynolds $\hspace{6cm} Re = \dfrac{\rho_c U_c L_c}{\mu_c}$

Suffixes

∞ Variable en el infinito sin perturbar

c Característica

d Gota (*droplet*)

e Borde de la capa límite (*edge*)

f Película de agua (*water film*)

w Agua (*water*)

Orbital elements

α Difusividad térmica $\hspace{7cm} \left[\dfrac{m^2}{s}\right]$

α_w Fracción volumétrica de agua en aire $\hspace{4.5cm} [---]$

$\bar{U}$ Vector velocidad de un cuerpo o fluido $\hspace{4cm} \left[\dfrac{m}{s}\right]]$

$\bar{u}$ Vector velocidad adimensional de un cuerpo o fluido $\hspace{2.5cm} [---]$

β Coeficiente de captación $[---]$

$\dot{m}$ Flujo másico $\left[\dfrac{kg}{s}\right]$

$\dot{m}'$ Flujo másico por unidad de área $\left[\dfrac{kg}{s}\dfrac{1}{m^2}\right]$

$\dot{Q}$ Flujo de calor $[W]$

$\dot{q}$ Flujo de calor por unidad de área $\left[\dfrac{W}{m^2}\right]$

μ Viscosidad dinámica de un fluido $[Pa \cdot s]$

ν Viscosidad cinemática de un fluido $\left[\dfrac{m^2}{s}\right]$

$\overline{\tau}_{wall}$ Esfuerzo viscoso de un fluido sobre una pared $[Pa]$

$\overline{c}_f$ Coeficiente de fricción viscosa sobre una pared $[---]$

ρ Densidad de un fluido $\left[\dfrac{kg}{m^3}\right]$

θ Temperatura absoluta adimensionalizada con la del punto triple $[---]$

$\tilde{T}$ Temperatura $[C]$

C_D Coeficiente de resistencia de un cuerpo $[---]$

C_p Calor específico a presión constante $\left[\dfrac{J}{kg\,K}\right]$

d Diámetro de las gotas $[\mu m]$

f Fracción de agua congelada $[---]$

h Espesor de una película de agua $[m]$

h_c Coeficiente de transferencia de calor por convección $\left[\dfrac{W}{m^2\,K}\right]$

k Conductividad térmica de un fluido $\left[\dfrac{W}{m\,K}\right]$

L Calor latente de un fluido $\left[\dfrac{J}{kg}\right]$

LWC Contenido en agua líquida, *liquid water content* $\left[\dfrac{kg}{m^3}\right]$

MVD Tamaño volumétrico medio de las gotas, *median volumetric diameter* $[\mu m]$

p Presión de un fluido $[Pa]$

$p_{v,sat}$ Presión de vapor de saturación $[Pa]$

r Factor de recuperación adiabática $[---]$

T Temperatura absoluta $[K]$

List of Figures

List of Tables

Relative dynamics around a near-circular reference orbit.

1.1 Introduction.

1.2 Motion model: Hill equations.

1.2.1 Differential equations of proximity relative motion.

As the proximity assumption ($\|\underline{r}\| << \|\underline{R}\|$) is quite widely common and valid for a fair range of operations, it is interesting to describe them here briefly, following [4]. Let us then consider the motion of two spacecrafts, namely, chief and deputy. The general equations of motion for each of them can be written as:

$$\textbf{Chief} \quad \Rightarrow \ddot{\underline{R}} \quad = -\mu \frac{R}{\|\underline{R}\|} + \underline{a}_{C,d} \tag{1.1}$$

$$\textbf{Deputy} \Rightarrow \ddot{\underline{R}} + \ddot{\underline{r}} = -\mu \frac{R+r}{\|\underline{R}+\underline{r}\|} + \underline{a}_{D,d} + \underline{a}_f \tag{1.2}$$

where $\underline{R}$ and $\underline{r}$ are the chief's absolute position vector and the deputy's relative position vector, respectively. $\underline{a}_{\bullet,d}$ is the disturbing acceleration on each spacecraft, while $\underline{a}_f$ denotes the thrust vector of the deputy. In order to facilitate the linearization, let us rewrite the orbital radius of the deputy as:

$$\|\underline{R}+\underline{r}\| = \left[(\underline{R}+\underline{r})^T(\underline{R}+\underline{r})\right]^{1/2} = \|\underline{R}\| \left(1 + 2\frac{R^T r}{\|\underline{R}\|^2} + \frac{\|r\|^2}{\|\underline{R}\|^2}\right)^{1/2}$$

then, the effect of the gravity field on the deputy can be expressed as:

$$\frac{R+r}{\|\underline{R}+\underline{r}\|^3} = \frac{R+r}{\|\underline{R}\|^3} = \left(1 + 2\frac{R^T r}{\|\underline{R}\|^2} + \frac{\|r\|^2}{\|\underline{R}\|^2}\right)^{-\frac{3}{2}}$$

Assuming that the relative distance is much smaller than the chief's orbital radius:

$$\frac{R+r}{\|R+r\|^3} \approx \frac{R+r}{\|R\|^3}\left[1 - \frac{3}{2}\left(2\frac{R^T r}{\|R\|^2} + \frac{\|r\|^2}{\|R\|^2}\right)\right] \approx \frac{1}{\|R\|^3}\left(R+r - 3\frac{R^T r}{\|R\|^2}R\right) \tag{1.3}$$

If we now substitute (1.3) in the difference (??) minus (1.1), we arrive to:

$$\ddot{r} = -\frac{\mu}{\|R\|^3}\left(r - 3\frac{R^T r}{\|R\|^2}R\right) + a_f + a_{D,d} - a_{C,d} \tag{1.4}$$

Experience shows it is convenient to express equation (1.4) in a chief-centered frame, for example, the LVLH frame (see section ??). This leads to the need of applying Coriolis' Theorem twice, so as to get the non-inertial effects derived from describing the motion in a rotating frame. The equations of motion take now the following form:

$$\ddot{r} = -\frac{\mu}{\|R\|^3}\left(r - 3\frac{R^T r}{\|R\|^2}R\right) - 2\omega \times \dot{r} - \dot{\omega} \times r - \omega \times (\omega \times r) + a_f + a_{D,d} - a_{C,d} \tag{1.5}$$

where ω is the target orbital rate. Let us now express each vector in the RTN frame:

$$\omega = \left\{\begin{array}{c} 0 \\ -\omega \\ 0 \end{array}\right\} \qquad R = \left\{\begin{array}{c} 0 \\ 0 \\ -R \end{array}\right\} \qquad r = \left\{\begin{array}{c} x \\ y \\ z \end{array}\right\} \tag{1.6}$$

leading to the next expressions for the terms in equation (1.5):

$$\omega \times \dot{r} = \left\{\begin{array}{c} \omega\dot{z} \\ 0 \\ \omega\dot{x} \end{array}\right\} \qquad\qquad \dot{\omega} \times r = \left\{\begin{array}{c} -\dot{\omega}z \\ 0 \\ \dot{\omega}x \end{array}\right\}$$

$$\omega \times (\omega \times r) = \left\{\begin{array}{c} -\omega^2 x \\ 0 \\ -\omega^2 z \end{array}\right\} \qquad\qquad r - 3\frac{R^T r}{\|R\|^2} = \left\{\begin{array}{c} x \\ y \\ -2z \end{array}\right\}$$

and introducing these results into (1.5), we arrive to:

$$
\left\{
\begin{array}{c}
\ddot{x} \\
\ddot{y} \\
\ddot{z}
\end{array}
\right\}
=
\left\{
\begin{array}{c}
-k\omega^{3/2}x + 2\omega\dot{z} + \dot{\omega}z + \omega^2 x \\
-k\omega^{3/2}y \\
2k\omega^{3/2}z - 2\omega\dot{x} - \dot{\omega}x + \omega^2 z
\end{array}
\right\}
+ \underline{a}_f + \underline{a}_{D,d} - \underline{a}_{C,d}
\tag{1.7}
$$

where k is a constant defined by

$$
\frac{\mu}{R^3} = \left(\frac{\mu}{h^{3/2}}\right) \equiv k\omega^{3/2} \Leftrightarrow k \equiv \frac{\mu}{h^{3/2}}
$$

and $h = \omega R^2$ is the chief's angular momentum. TO BE CONTINUED, MATRIX FORM OF HILL EQUATIONS. ALSO ADD VECTOR NOTATION OF EACH. RTN FRAME FOR HCW?

1.2.2 Hill equations.

1.3 Solutions of Hill equations.

1.3.1 Approaches.

1.3.2 Direct numerical integration.

1.3.3 Clohessy-Wiltshire solution.

1.3.4 State transition matrix propagation.

1.3.4.1 Jordan canonical decomposition.

1.3.5 Results: Comparison against High-Fidelity.

1.3.5.1 Scenario 1: XXXXXX

1.3.5.2 Scenario 2: XXXXXX

1.3.5.3 Scenario 3: XXXXXX

1.4 Orbit safety in near-circular orbits.

1.4.1 Orbit safety concept.

Orbit or trajectory safety can be understood as how protected from danger or risk our spacecraft set is. It is essentially a kinematic condition, being closely related to the notions of relative position and distance, and how these vary over time. Both branches of relative motion (*i.e.* rendez-vous and formation flying) are subject to this concept.

One of the biggest concerns about orbit safety is trajectory uncertainty. If we knew the exact position of each spacecraft, safety margins could be lowered down to almost zero, but unfortunately, that is not the case. For this reason, distance margins have to be established. As we have seen,

there are three basic components in relative motion: radial, along-track and cross-track. The most susceptible one to estimation errors is the along-track component, due to the high influence of the semimajor axis on the angular rate, thus on the angular position [7]. Hence, along-track uncertainty will always tend to be much higher than either radial or cross-track.

With this fact in mind, it seems logical to try and separate the spacecrafts in radial or cross-track components, as motion can be more accurately predicted in those directions. It is here where the eccentricity/inclination vector separation concept raises, as an approach to describe the periodic relative motion that takes place in said components. In the following section, its grounds and applications will be discussed, both in general terms and applied to near-circular reference orbits.

1.4.2   Eccentricity-inclination vector separation strategy.

1.4.2.1   Eccentricity and inclination vectors.

The eccentricity and inclination vectors constitute an interesting way to parametrize relative motion. This description was firstly introduced by Eckstein [7], aimed at geostationary orbits. Later on, it was extended to proximity LEO operations [**Montenbruck·DAmico**], which is today's main scope of application.

This approach to orbit safety will be treated recurrently along the thesis, being progressively extended as the orbits grow in complexity. In this section, the basics of this concept will be described, starting with the parametrization of proximity relative motion in terms of the eccentricity and inclination vectors (see appendix **??**). After that, the two setups of $\delta\underline{e}$ and $\delta\underline{i}$ are discussed.

1.4.2.2   Linearized effect of δe and δi in relative position.

Our target is to obtain an expression which relates the eccentricity and inclination vector components to the radial, along-track and cross-track distances. This can be done by applying some transformations to the already available Keplerian OE set to RTN (see **??**), or through a geometric analysis of the motion. As the first one is almost trivial (considered said section), let us proceed with the second one, explained in more detail in [**DAmico·Montenbruck**]:

I. Effect of relative eccentricity vector $\delta\underline{e}$.

The relative eccentricity vector accounts for the variation in the eccentricity value and the argument of perigee. Assuming no other variation in any element, it can be projected on the chief's orbital plane,

leading to:

$$\underline{e} = \left\{ \begin{array}{c} e_x \\ e_y \end{array} \right\} = e \left\{ \begin{array}{c} \cos\omega \\ \sin\omega \end{array} \right\} \Rightarrow \delta\underline{e} = \left\{ \begin{array}{c} \delta e_x \\ \delta e_y \end{array} \right\} = \delta e \left\{ \begin{array}{c} \cos\varphi \\ \sin\varphi \end{array} \right\}$$

The relative eccentricity has an effect on the in-plane motion. That is to say, on the radial and along-track components. In order to get these, we must first derive some expressions for the orbital radius r and the difference $\theta - M$.

The orbital radius for near-circular orbits ($|e| << 1$) can be expressed as:

$$\frac{r}{a} = 1 - e\cos E \approx 1 - e\cos M = 1 - e\cos(\lambda - \omega) = 1 - e\cos\omega\cos\lambda + e\sin\lambda\sin\omega$$

$$\frac{r}{a} \approx 1 - e_x\cos\lambda - e_y\sin\lambda \qquad (1.8)$$

where λ is the mean argument of latitude, which embodies the time-varying element of the E/I element set. The second auxiliary expression $\theta - M$ can be obtained in many handbooks, by looking for the series expansion of the mean anomaly in terms of the true [20]:

$$M = \theta + 2\sum_{n=1}^{\infty}(-1)^n\left(\frac{1}{n} + \sqrt{1-e^2}\right)\beta^n\sin n\theta \underset{e<<1}{\approx} \theta - 2e\sin\theta$$

$$\theta - M = 2e\sin M = 2e\sin(\lambda - \omega) = 2e(\sin\lambda\cos\omega - \cos\lambda\sin\omega) = 2e_x\sin\lambda - 2e_y\cos\lambda \qquad (1.9)$$

Assuming that both spacecrafts have the same mean argument of latitude and semimajor axis, the radial and along-track distance (δr_R, δr_T) between chief and deputy are due to (a) the difference in orbital radius δr and (b) the difference in true argument of latitude $\delta u = \delta\theta + \delta\omega$. With this in mind, let us construct a graphical representation of the situation, shown in 1.1:

DUMMY FIGURE

Figure 1.1: Effect of δr and δu in radial and along-track distances.

The angle α can be developed in terms of known magnitudes, that is:

$$\alpha = u_2 - u_1 = (\lambda_2 - \lambda_1) + (\theta_2 - M_2) - (\theta_1 - M_1)$$

I.A. Effect of $\delta\underline{e}$ in δr_R.

Radial distance can be derived from figure 1.1 as:

$$\delta r_R = r_2 \cos\alpha - r_1 = r_2 \cos(u_2 - u_1) - r_1 = r_2 \cos(\lambda_2 - \lambda_1 + \theta_2)$$

In virtue of equation (1.8):

$$\delta r_R = r_2 \cos\alpha - r_1 \approx a\left(e_1 \cos M_1 - e_2 \cos M_2\right)$$
$$\Rightarrow \frac{\delta r_R}{a} = e_1\left(\cos\lambda\cos\omega_1 - \sin\lambda\sin\omega_1\right) - e_2\left(\cos\lambda\cos\omega_2 - \sin\lambda\sin\omega_2\right) = \cos\lambda\left(e_{x1} - e_{x2}\right) - \sin\lambda\left(e_{y1} - e_{y2}\right)$$
$$\Rightarrow \frac{\delta r_R}{a}\Big|_{\delta e} \approx -\delta e_y \sin\lambda - \delta e_x \cos\lambda$$

$$(1.10)$$

I.B. Effect of $\delta\underline{e}$ in δr_T.

With the same assumptions as before, t

I.B. Effect of $\delta\underline{e}$ in δr_T.

1.4.2.3   Collision avoidance: $\delta\underline{e}/\delta\underline{i}$ separation.

Parallel configuration.

Antiparallel configuration.

Relative dynamics around elliptic reference orbits.

2.1 Introduction.

In the previous chapter, the Clohessy-Wiltshire set of equations of motion has been analyzed. Getting them from Newton's law required the fulfillment of two assumptions. Firstly, the distance between deputy and chief must be negligible compared to either spacecraft's orbital radius. This is usually the case when dealing both with formation flying and rendez-vous maneuvers. The second assumption is that both orbits are near-circular ($e << 1$), which is not as acceptable as the first one. This is specially relevant on formation flying, as the timescale is usually large enough to experience sensible deviations.

Conceptually, there are some obvious differences between near-circular and eccentric orbits. First of all, orbital radius varies over time, which means that, at every point, the spacecraft is radially closing or moving away from the central body (*i.e.* the Earth). But more importantly, the angular velocity is no longer constant, which means that the non-inertial effects when analyzing the relative motion are not constant. That will surely make it harder to get analytical expressions, though through some simplifications, it may be done.

For this reason, several motion models for elliptic orbits have been developed [1]. Both linear and nonlinear models are present in the literature, though the first ones are the most usually employed. Tschauner and Hempel [2] developed a linear, first-order model via the truncation of the Taylor series expansion of the differential gravity. The so-called Tschauner-Hempel equations were widely used at the time, as they are consistent with the Hill/Clohessy-Wiltshire (HCW) model. Nonetheless, they were subsequently improved, due to the existence of singularities in the in-plane motion. Carter [3] provides a non-singular solution for this issue.

Instead of these solutions, the motion model used for elliptic, unperturbed orbits in this thesis is one developed by Yamanaka and Ankersen [4] (YA onwards). It results in a fairly simpler STM, which

is generally considered the state-of-the-art solution for linear propagation of the relative position and velocity in eccentric orbits. It will actually be used in the PROBA-3 mission, which flies in a highly elliptical orbit.

During this chapter, we will firstly develop YA's approach for the motion model and their proposed solution for it. This enables in turn to develop the YA STM, which will be duly tested with their own scenarios. Lastly, orbit safety concerns will be approached, extending the prior knowledge from near-circular orbits to arbitrarily elliptical, as done by Peters and Noomen [5].

2.2   Motion model and STM.

2.2.1   Simplification of equations of motion: YA solution.

As developed in section 1.2.1, the differential equations for proximity relative motion are:

$$
\left\{ \begin{array}{c} \ddot{x} \\ \ddot{y} \\ \ddot{z} \end{array} \right\} = \left\{ \begin{array}{c} -k\omega^{3/2}x + 2\omega\dot{z} + \dot{\omega}z + \omega^2 x \\ -k\omega^{3/2}y \\ 2k\omega^{3/2}z - 2\omega\dot{x} - \dot{\omega}x + \omega^2 z \end{array} \right\} + \underline{a}_f + \underline{a}_{D,d} - \underline{a}_{C,d} \tag{2.1}
$$

In this chapter, we will focus solely on the unperturbed version of this problem, that is, $\underline{a}_f = \underline{a}_{D,d} = \underline{a}_{C,d} = \underline{0}$. A slightly more general approach is to assume that, if dealing with perturbed motion, the perturbation acceleration is equal on either body. The main difference now with respect to Hill equations (CITE HILL EQUATIONS) is that the angular rate ω is now time-varying, whereas before it was constant ($\omega = n = $ const.). This fact completely changes the character of the mathematical problem: the coefficient matrix is no longer constant.

It is here where Yamanaka and Ankersen, following Carter's approach, implement two changes. Firstly, chief's true anomaly θ is adopted as the independent variable instead of time. That changes the derivative definition, and for a certain variable ξ, the conversion from time to true anomaly derivatives is as follows:

$$
\begin{cases} \dfrac{d\xi}{dt} = \dfrac{d\xi}{d\theta}\dfrac{d\theta}{dt} = \omega\dfrac{d\xi}{d\theta} & \Rightarrow \dot{\xi} = \omega\xi' \tag{2.2a} \\[2ex] \dfrac{d^2\xi}{dt^2} = \dfrac{d}{dt}\left(\dfrac{d\xi}{dt}\right) = \omega\dfrac{d\omega}{d\theta}\dfrac{d\xi}{d\theta} + \omega^2\dfrac{d^2\xi}{dt^2} \Rightarrow \ddot{\xi} = \omega^2\xi'' + \omega\omega'\xi' \tag{2.2b} \end{cases}
$$

where ω' is calculated by simply using the angular momentum definition:

$$
\omega = \frac{h}{R^2} = \frac{h}{p^2}\left(1 + e\cos\theta\right)^2 = k^2\rho^2 \Rightarrow \omega\prime = 2k^2\rho\rho' = -2k^2 e\sin\theta\rho \tag{2.3}
$$

Substituting (**??**), (**??**) and (**??**) into (**??**) yields:

$$
\begin{cases}
\rho x'' - 2e \sin\theta\, x' - e \cos\theta\, x & = 2\rho z' - 2e \sin\theta\, z & \text{(2.4a)} \\[2mm]
\rho y'' - 2e \sin\theta\, y' & = -y & \text{(2.4b)} \\[2mm]
\rho z'' - 2e \sin\theta\, z' - (3 + e \cos\theta) z = -2\rho x' + 2e \sin\theta\, x & & \text{(2.4c)}
\end{cases}
$$

Once this change of variable has been applied, the following transformation is performed:

$$
\left\{
\begin{array}{c}
\widetilde{x} \\
\widetilde{y} \\
\widetilde{z}
\end{array}
\right\}
= (1 + e \cos\theta)
\left\{
\begin{array}{c}
x \\
y \\
z
\end{array}
\right\}
\tag{2.5}
$$

which, if substituted in (**??**), lead to the rather simple following set of equations:

$$
\begin{cases}
\widetilde{x}'' = 2\widetilde{z}' & \text{(2.6a)} \\[2mm]
\widetilde{y}'' = -\widetilde{y} & \text{(2.6b)} \\[2mm]
\widetilde{z}'' = 3\dfrac{\widetilde{z}}{\rho} - 2\widetilde{x}' & \text{(2.6c)}
\end{cases}
$$

The initial conditions that complete the initial value problem (IVP) can be written as:

$$
\left\{
\begin{array}{c}
\widetilde{x} \\
\widetilde{y} \\
\widetilde{z}
\end{array}
\right\}
(\theta_0) =
\left\{
\begin{array}{c}
\widetilde{x}_0 \\
\widetilde{y}_0 \\
\widetilde{z}_0
\end{array}
\right\}
= (1 + e \cos\theta_0)
\left\{
\begin{array}{c}
x_0 \\
y_0 \\
z_0
\end{array}
\right\}
$$

Solution of the simplified set of equations.

It is rather obvious that equations (**??**), (**??**), (**??**) feature a decoupling between in-plane components (x-z) and out-of-plane (y). The latter can easily be solved as:

$$
\widetilde{y} = K_{y1} \sin\theta + K_{y2} \cos\theta
\tag{2.7}
$$

while for the in-plane motion, equation (**??**) must be first integrated, then introduced into (**??**), yielding:

$$
\widetilde{z}'' + \left(4 - \frac{3}{\rho}\right)\widetilde{z} = -2K_{x1}
\tag{2.8}
$$

with $\widetilde{x}$ is calculated from $\widetilde{z}$ as:

$$\widetilde{z}' = 2\widetilde{z} + K_{x1} \tag{2.9}$$

where K_i is the set of integration constants, derived from the prescribed initial conditions. The relation between them will be later described.

The task at hand now is to solve (??). Yamanaka and Ankersen propose a new solution to it, whose mathematical development is explained in [4]. Bottom line is that, the solution for $\widetilde{z}$ is:

$$\widetilde{z} = K_{z1}\rho\sin\theta + \left(K_{z2} - \frac{K_{x1}}{e}\right)\rho\cos\theta - K_{z2}e\left(2 - 3e\rho\sin\theta J\right) \tag{2.10}$$

where:

$$J = k^2(t - t_0)$$

Substituting into (??) and integrating:

$$\widetilde{x} = K_{x2} - K_{z1}\cos\theta\left(\rho + 1\right) + \left(K_{z2} - \frac{K_{x1}}{e}\right)\sin\theta\left(\rho + 1\right) - 3K_{z2}e\rho^2 J \tag{2.11}$$

Redefining the integral constants for simplicity as:

$$K_1 \equiv K_{x2} \qquad K_2 \equiv K_{z1} \qquad K_3 = \left(K_{z2} - \frac{K_{x1}}{e}\right) \qquad K_4 = -K_{z2}e$$

and using the following simplified notation

$$s = \rho\sin\theta \qquad c = \rho\cos\theta$$

the solution of the in-plane dynamics turns fairly simpler:

$$\begin{cases} \widetilde{x} = K_1 - K_2 c\left(1 + \dfrac{1}{\rho}\right) + K_3 s\left(1 + \dfrac{1}{\rho}\right) + 3K_4\rho^2 J & \text{(2.12a)} \\[2mm] \widetilde{z} = K_2 s + K_3 c + K_4\left(2 - 3es J\right) & \text{(2.12b)} \end{cases}$$

By simply differentiating the latter equations, we can obtain the in-plane velocity components. Considering both position and velocity, a simple matrix form can be achieved:

$$
\left\{
\begin{array}{c}
\widetilde{x} \\
\widetilde{z} \\
\widetilde{v}_x \\
\widetilde{v}_z
\end{array}
\right\}
=
\left[
\begin{array}{cccc}
1 & -c(1+\rho^{-1}) & s(1+\rho^{-1}) & 3\rho^2 J \\
0 & s & c & (2-3esJ) \\
0 & 2s & 2c-e & 3(1-2esJ) \\
0 & s' & c' & -3e(s'J+s/\rho^2)
\end{array}
\right]
\left\{
\begin{array}{c}
K_1 \\
K_2 \\
K_3 \\
K_4
\end{array}
\right\}
\equiv \Phi_\theta|_{IP}\, \underline{K}_{IP} \qquad (2.13)
$$

where:

$$
s' = \cos\theta + e\cos 2\theta \qquad c' = -(\sin\theta + e\sin 2\theta)
$$

The out-of-plane problem can be expressed in this form as well:

$$
\left\{
\begin{array}{c}
\widetilde{y} \\
\widetilde{v}_y
\end{array}
\right\}
=
\left[
\begin{array}{cc}
\cos\theta & \sin\theta \\
-\sin\theta & \cos\theta
\end{array}
\right]
\left\{
\begin{array}{c}
\widetilde{y}_0 \\
\widetilde{v}_{y0}
\end{array}
\right\}
\equiv \Phi_\theta|_{OOP}\, \underline{K}_{OOP} \qquad (2.14)
$$

2.2.2 YA STM and integration constants.

Our target is to obtain a state transition matrix, that is, a matrix which when fed a state vector at a given time, returns the state vector at a latter epoch. Generally speaking, said entity is built as:

$$
\Phi^\theta_{\theta_0} = \Phi_\theta \Phi^{-1}_{\theta_0} \Rightarrow \underline{x}(\theta) = \Phi^\theta_{\theta_0}\underline{x}(\theta_0)
$$

where θ can be substituted by any independent variable, such as time. Yamanaka and Ankersen propose to merge the second part of the STM and the initial state vector, leading to the so-called pseudoinitial state vector, defined by:

$$
\overline{x}_0 = \Phi^\theta_{\theta_0}\underline{x}(\theta_0)
$$

which is also called the YA element set. With this in mind, our target now is to obtain both matrices, which in fact can be built from the in- and out-of-plane parts, previously defined in (??) and (??).

2.2.2.1   In-plane motion.

The first component Φ_θ was already defined as (**??**):

$$
\Phi_\theta|_{IP} =
\begin{bmatrix}
1 & -c(1+\rho^{-1}) & s(1+\rho^{-1}) & 3\rho^2 J \\
0 & s & c & (2-3esJ) \\
0 & 2s & 2c-e & 3(1-2esJ) \\
0 & s' & c' & -3e(s'J + s/\rho^2)
\end{bmatrix}
\tag{2.15}
$$

In order to get $\Phi_{\theta_0}|_{IP}^{-1}$, let us note that $J(\theta_0) = J(t_0) = 0$. Once applied that, the inverse is not so hard to compute, namely:

$$
\Phi_{\theta_0}|_{IP}^{-1} = \frac{1}{1-e^2}
\begin{bmatrix}
1-e^2 & 3e(s/\rho)\left(1+\rho^{-1}\right) & -es\left(1+\rho^{-1}\right) & 2-ec \\
0 & -3(s/\rho)\left(1+e^2/\rho\right) & s\left(1+\rho^{-1}\right) & c-2e \\
0 & -3\left(e+c/\rho\right) & c\left(1+\rho^{-1}\right)+e & -s \\
0 & 3\rho+e^2-1 & -\rho^2 & es
\end{bmatrix}_{\theta_0}
\tag{2.16}
$$

2.2.2.2   Out-of-plane motion.

The out-of-plane equations require a less cumbersome manipulation. As we already have the full STM in (**??**), we have to first divide it into the two subcomponents by substituting θ for $\theta - \theta_0$. Then, using trigonometric relations for the sum of sines and cosines, it is easy to pull both matrices apart as:

$$
\Phi_{\theta_0}^\theta =
\begin{bmatrix}
\cos(\theta-\theta_0) & \sin(\theta-\theta_0) \\
-\sin(\theta-\theta_0) & \cos(\theta-\theta_0)
\end{bmatrix}
=
\begin{bmatrix}
\cos\theta & \sin\theta \\
-\sin\theta & \cos\theta
\end{bmatrix}
\begin{bmatrix}
\cos\theta_0 & -\sin\theta_0 \\
\sin\theta_0 & \cos\theta_0
\end{bmatrix}
\equiv \Phi_\theta \Phi_{\theta_0}^{-1}
\tag{2.17}
$$

This expression could have also been reached similarly to the in-plane counterpart.

2.2.2.3 Full matrices.

By simply but carefully placing the elements of (??), (??), and (??) in a 6x6 matrix, we can finally reach the full matrices as:

$$
\Phi_\theta =
\begin{bmatrix}
1 & 0 & -c(1+\rho^{-1}) & s(1+\rho^{-1}) & 0 & 3\rho^2 J \\
0 & \cos\theta & 0 & 0 & \sin\theta & 0 \\
0 & 0 & s & c & 0 & 2-3esJ \\
0 & 0 & 2s & 2c-e & 0 & 3(1-2esJ) \\
0 & -\sin\theta & 0 & 0 & \cos\theta & 0 \\
0 & 0 & s' & c' & 0 & -3e(s'J+s/\rho^2)
\end{bmatrix}
\tag{2.18a}
$$

$$
\Phi_{\theta_0}^{-1} = \frac{1}{1-e^2} \times
$$
$$
\begin{bmatrix}
1-e^2 & 0 & 3e(s/\rho)(1+\rho^{-1}) & -es(1+\rho^{-1}) & 0 & 2-ec \\
0 & (1-e^2)\cos\theta & 0 & 0 & -(1-e^2)\sin\theta & 0 \\
0 & 0 & -3(s/\rho)(1+e^2/\rho) & s(1+\rho^{-1}) & 0 & c-2e \\
0 & 0 & -3(c/\rho+e) & c(1+\rho^{-1})+e & 0 & -s \\
0 & (1-e^2)\sin\theta & 0 & 0 & (1-e^2)\cos\theta & 0 \\
0 & 0 & 3\rho+e^2-1 & -\rho^2 & 0 & es
\end{bmatrix}
\tag{2.18b}
$$

2.2.2.4   Pseudo-initial state vector.

Finally, let us compute the so-called pseudoinitial conditions as defined before, namely:

$$
\left\{
\begin{array}{c}
\overline{x}_0 \\
\overline{y}_0 \\
\overline{z}_0 \\
\overline{v}_{x0} \\
\overline{v}_{y0} \\
\overline{v}_{z0}
\end{array}
\right\} = \Phi_{\theta_0}^{-1} \widetilde{\underline{x}}_0 = \frac{1}{1-e^2} \times
$$

$$
\begin{bmatrix}
1-e^2 & 0 & 3e(s/\rho)(1+\rho^{-1}) & -es(1+\rho^{-1}) & 0 & 2-ec \\
0 & (1-e^2)C\theta & 0 & 0 & -(1-e^2)S\theta & 0 \\
0 & 0 & -3(s/\rho)(1+e^2/\rho) & s(1+\rho^{-1}) & 0 & c-2e \\
0 & 0 & -3(c/\rho+e) & c(1+\rho^{-1})+e & 0 & -s \\
0 & (1-e^2)S\theta & 0 & 0 & (1-e^2)C\theta & 0 \\
0 & 0 & 3\rho+e^2-1 & -\rho^2 & 0 & es
\end{bmatrix}
\left\{
\begin{array}{c}
\widetilde{x}_0 \\
\widetilde{y}_0 \\
\widetilde{z}_0 \\
\widetilde{v}_{x0} \\
\widetilde{v}_{y0} \\
\widetilde{v}_{z0}
\end{array}
\right\} \quad (2.19)
$$

where $C = \cos$ and $S = \sin$. Nonetheless, the right hand side vector $\widetilde{\underline{x}}_0$ is actually a transformation of a genuine LVLH state vector (see (**??**)), which is the true inputs of our relative dynamics problem. For that reason, it is necessary to map the transformed state vector $\widetilde{\underline{x}}$ from and to the original one $\underline{x}$. This is done through the matrix T_θ as follows:

$$
\widetilde{\underline{x}} = T_\theta \underline{x} \Rightarrow
\left\{
\begin{array}{c}
\widetilde{r} \\
\widetilde{v}
\end{array}
\right\} =
\begin{bmatrix}
\rho \mathbb{I}_{3x3} & \mathbb{O}_{3x3} \\
-e\sin\theta \mathbb{I}_{3x3} & \dfrac{1}{k^2\rho} \mathbb{I}_{3x3}
\end{bmatrix}
\left\{
\begin{array}{c}
r \\
v
\end{array}
\right\} \quad (2.20)
$$

The combination of (??) and (??) lead to a transformation between a LVLH state vector and the so-called Yamanaka-Ankersen element set, through the transformation matrix $T_{LVLH \to YA}$:

$$\overline{x} \equiv \underline{x}_{YA} = \Phi_{\theta_0}^{-1} T_\theta \underline{x}_{LVLH} = \frac{1}{1-e^2} \times$$

$$\begin{bmatrix} 1-e^2 & 0 & 3e(s/\rho)(1+\rho^{-1}) & -es(1+\rho^{-1}) & 0 & 2-ec \\ 0 & (1-e^2)\cos\theta & 0 & 0 & -(1-e^2)\sin\theta & 0 \\ 0 & 0 & -3(s/\rho)(1+e^2/\rho) & s(1+\rho^{-1}) & 0 & c-2e \\ 0 & 0 & -3(c/\rho+e) & c(1+\rho^{-1})+e & 0 & -s \\ 0 & (1-e^2)\sin\theta & 0 & 0 & (1-e^2)\cos\theta & 0 \\ 0 & 0 & 3\rho+e^2-1 & -\rho^2 & 0 & es \end{bmatrix} \times$$

$$\begin{bmatrix} \rho & 0 & 0 & & & \\ 0 & \rho & 0 & & \mathbb{O}_{3x3} & \\ 0 & 0 & \rho & & & \\ -e\sin\theta & 0 & 0 & \dfrac{1}{k^2\rho} & 0 & 0 \\ 0 & -e\sin\theta & 0 & 0 & \dfrac{1}{k^2\rho} & 0 \\ 0 & 0 & -e\sin\theta & 0 & 0 & \dfrac{1}{k^2\rho} \end{bmatrix} \underline{x}_{LVLH} \tag{2.21}$$

2.2.2.5 Solution scheme.

The target is to compute the relative state vector at a certain time epoch, given the following inputs:

- $\underline{x}_{LVLH}|_0$: Initial LVLH relative state vector (see section **??**).

- $\underline{KOE}_C|_0$: Initial chief's Keplerian OE set (see section **??**).

- t: Time elapsed from the initial time epoch to the desired one.

This is, as explained in appendix **??**, the usual workflow for orbit propagation. With all the operations and transformations previously described, this process is graphically described in **??**.

2.2.3 Results: Comparison with HCW and Hi-Fi propagation.

Once we have defined the complete model for orbit propagation, it is turn to discuss how does it compare with respect to the previous solution (HCW) and the High-Fidelity propagation. The workflows for both of these approach are available at **REF HCW DIAGRAM** and **REF HIFI**
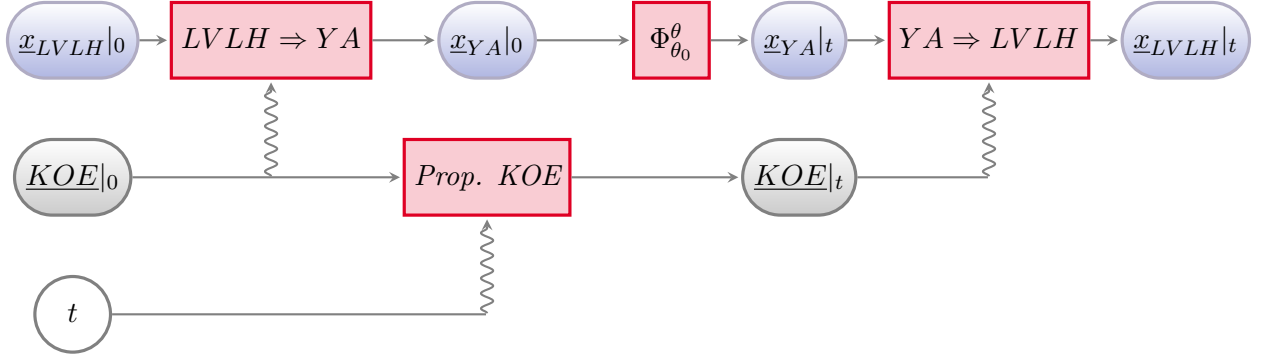
Figure 2.1: Workflow of the propagation with YA STM.

DIAGRAM.

Now, let us define (rather cite) a scenario to test this method. In order to be able to compare the results with the method source, we will use the scenarios defined by Yamanaka and Ankersen [4]. As we know, if no body-dependent perturbations are considered, a scenario is completely defined by:

- Chief's reference orbit (Keplerian OEs)

- Deputy's relative position and velocity with respect to chief (LVLH frame)

- Propagation values: Time elapsed and numerical method for high-fidelity propagation(algorithm, timestep . . .)

In this case, Yamanaka and Ankersen define them as:

Parameter	Value
Chief's orbit	
Eccentricity	$e_1 = 0.1$, $e_2 = 0.7$
Perigee height	$h_p = 500$ km
Inclination	$i = 30°$
RAAN	$\Omega = 0°$
Argument of perigee	$\omega = 0°$
True anomaly at $t = 0$	$\theta = 45°$
Deputy's relative position (LVLH frame)	
Initial position	$\{x, y, z\} = [100, 10, 10]$ m
Initial velocity	$\{\dot{x}, \dot{y}, \dot{z}\} = [0.1, 0.1, 0.1]$ m/s
Propagation parameters	
Propagation time	$N_{orbits} = 2$
Numerical method	Fourth order Runge-Kutta

Table 2.1: Testing scenarios for YA STM [4].

Nonetheless, we must get the set of Keplerian OEs as defined in **??**. Firstly, let us compute the semimajor axis from the perigee height h_p as:
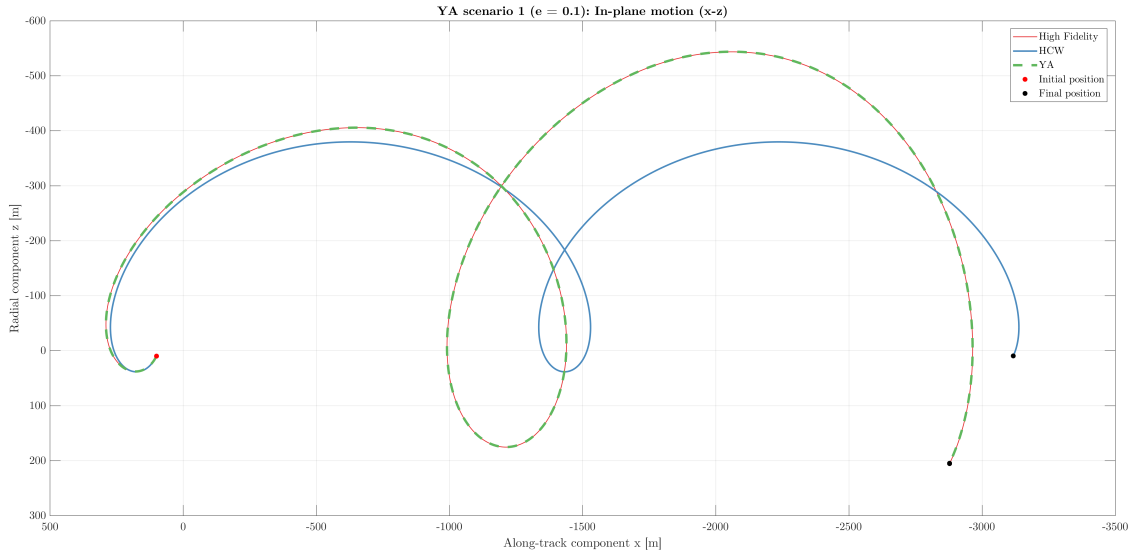
$$h_p = a(1 - e) \Rightarrow a = \frac{h_p}{1 - e}$$

Secondly, the mean anomaly is computed from the true anomaly and the eccentricity, as explained in **REF MEAN2TRUE**. Then, the Keplerian OEs for both scenarios are:
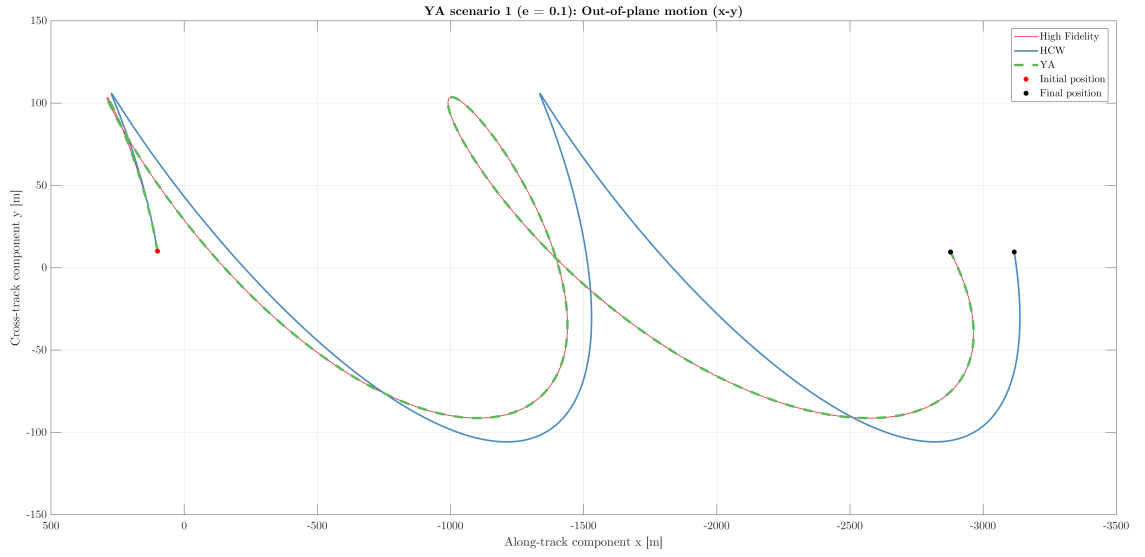
$$\begin{cases} \underline{KOE}_1 = (7.61861333 \cdot 10^6, \ 0.1, \ \pi/6, \ 0, \ 0, \ 0.65125326) & [\text{m}, \ -, \ \text{rad}, \ \text{rad}, \ \text{rad}, \ \text{rad}] \quad (2.22\text{a}) \\ \underline{KOE}_2 = (2.28558400 \cdot 10^7, \ 0.7, \ \pi/6, \ 0, \ 0, \ 0.10811191]) & [\text{m}, \ -, \ \text{rad}, \ \text{rad}, \ \text{rad}, \ \text{rad}] \quad (2.22\text{b}) \end{cases}$$

Let us now proceed with the result evaluation.
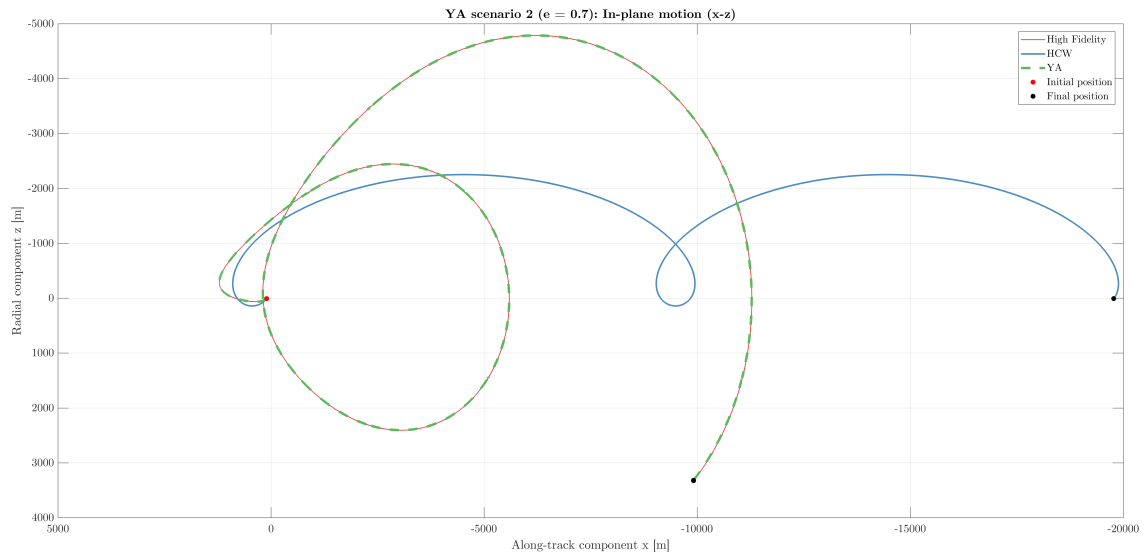
2.2.3.1 Scenario 1: $e = 0.1$.
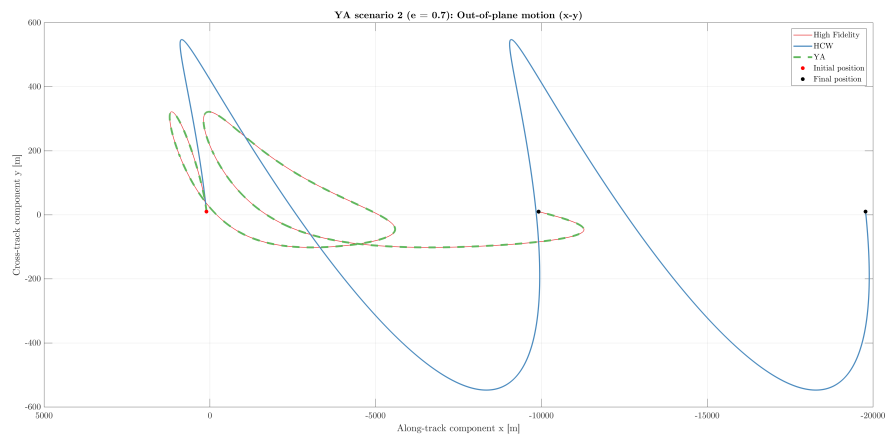

(a) In-plane motion.

(b) Out-of-plane motion.

Figure 2.2: Scenario 1($e = 0.1$): Comparison between Hi-Fi, HCW and YA.

2.2.3.2   Scenario 2: $e = 0.7$.

(a) In-plane motion.

(b) Out-of-plane motion.

Figure 2.3: Scenario 2 ($e = 0.7$): Comparison between Hi-Fi, HCW and YA.

2.3   Orbit safety in eccentric, unperturbed orbits.

2.3.1   Generalized eccentricity/inclination vectors separation.

2.3.2   General trajectories and safe orbits.

Absolute and relative orbital element sets.

A.1   Introduction.

The description of a spacecraft's state is done via a **state vector**. While it can include several variables with other purposes (*e.g.* filtering), its only information throughout this thesis is the position and velocity. There are two main ways to describe them:

A. Through **cartesian coordinates**

B. Through **orbital elements**

While the first option yields a very explicit and graphic-ready description, the second one usually has two advantages over it. Firstly, orbital elements are generally more intuitive about both the orbit and the position on it. Secondly, as orbital elements are generally slow-varying, they allow for a bigger integration timestep without losing accuracy. This is quite clear when studying keplerian motion, as most of the elements remain constant. Variational formulation and Hamilton-Jacobi theory (with the notion of changing variables as the full solution of a problem) relate to this fact.

Throughout this thesis, several sets of orbital elements have been used. The goal of this appendix is to clarify on the definition and differences between them. Absolute orbital elements (OEs) will be described first, followed by relative OEs (ROEs).

A.2   Absolute element sets.

A.2.1   Workflow for transformations between absolute element sets.

Consider two different sets of OEs, denoted by $\underline{OE}$ and $\widetilde{\underline{OE}}$. The transformation function $\boldsymbol{G}_{OE \to \widetilde{OE}}$ between them is defined by:

$$\widetilde{\underline{OE}} = \boldsymbol{G}_{OE \to \widetilde{OE}}(\underline{OE}) \tag{A.1}$$

A numerous amount of element sets have been historically defined. Nevertheless, some of them are much more commonly used than others. Although we will restrain ourselves to a short number of sets (say n), the number of transformations becomes arduously large as n increases ($n(n-1)$).

In order to reduce the number of transformation functions $\boldsymbol{G}$, let us use the later defined Keplerian OEs (KOEs) as a pivot, that is, building only transformations to and from KOEs. This will in turn reduce the number of required functions to $2n$. The Keplerian set also has a further advantage: as it is the classical element set, almost every other set is defined explicitly in terms of it, so that transformations to and from them can easily be derived. A simple, graphical explanation of this is shown in figure **??**.

Figure A.1: Workflow for transforming between two arbitary absolute element sets.

A.2.2 Element sets.

A.2.2.1 Keplerian orbital elements (KOE).

The Keplerian set of OEs (KOE) is one of the most widely used and classic options. While the last element may change from author to author, an usual definition is the following:

$$
\begin{cases}
a & \equiv \quad \text{Semimajor axis} & [L] \\
e & \equiv \quad \text{Eccentricity} & [--] \\
i & \equiv \quad \text{Inclination} & [rad] \\
\Omega \text{ or } RAAN & \equiv \quad \text{Right ascension of the ascending node} & [rad] \\
\omega & \equiv \quad \text{Argument of periapsis} & [rad] \\
M & \equiv \quad \text{Mean anomaly} & [rad]
\end{cases}
\tag{A.2}
$$

The last element commonly varies across literature, being substituted by the true anomaly θ; or, when tackling the variation of orbital parameters, by the mean anomaly at $t = 0$ (M_0) or the perigee time T_0 [6]. Mean anomaly is used due to the simplicity of its unperturbed variational equation, as it has a constant rate (denoted by n). The geometrical meaning and definition of these elements is out from the scope of this thesis. Nonetheless, figure **??** shows a simple geometrical drawing of the involved angles.
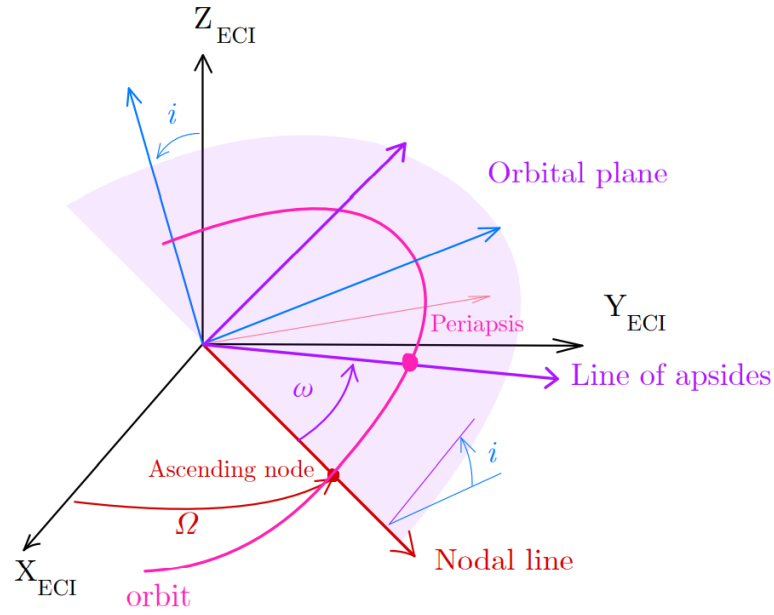
Figure A.2: Frame rotation from inertial to perifocal frame.

As it is seen in the figure before, the Keplerian elements become singular in two cases:

A. If the **inclination** is null, the orbital plane is coincident with the inertial reference (ECI x-y) plane. The ascending node is hence undefined in this case.

B. If the **eccentricity** is null, the periapsis is not defined, as it is the nearest point of the orbit around the central body. Thus, there is no angle defining its position, making the argument of periapsis nonsingular.

These singularities are unfortunately quite common in orbit design. They correspond respectively with equatorial and circular orbits. In order to avoid this behaviour, many different elements sets have been defined. Wiesel [6] shows an intuitive approach in chapter 2.10, solving either problem with a graphic approach.

A.2.2.2   Eccentricity/inclination vectors orbital elements (EIOE).

This set, originally defined for geostationary orbits in absolute terms [7], is used mainly as a relative OE set. Though it is actually not used along this thesis, its definition is helpful for introducing the common relative counterpart. In any case, let us proceed with the eccentricity and inclination vectors concept.

Eccentricity vector

The notion of the eccentricity vector is quite basic, as it is, when in unperturbed motion, a constant of the dynamic system. It is defined as the eccentricity-sized vector pointing towards the perigee. Nonetheless, for this purpose, the eccentricity vector is defined as [8]:

$$
\underline{e} = \left\{ \begin{array}{c} e_x \\ \\ e_y \end{array} \right\} = e \left\{ \begin{array}{c} \cos \varpi \\ \\ \sin \varpi \end{array} \right\} \tag{A.3}
$$

where the argument of perigee ω might be substituted with the sum $\omega + \Omega$ [as in 7]. A graphical representation can be seen later in the relative definition **??**. As it arises from (**??**), it substitutes the eccentricity and argument of perigee from the Keplerian OE set.

Inclination vector

The inclination vector is perpendicular to the orbital plane, similarly to the angular momentum, but inclination-sized. It is defined by its components as [7]:

$$
\underline{i} = \left\{ \begin{array}{c} i_x \\ \\ i_y \end{array} \right\} = i \left\{ \begin{array}{c} \cos \Omega \\ \\ \sin \Omega \end{array} \right\}
$$

The graphical interpretation is not as straightforward as for the eccentricity vector. Nonetheless, we are only interested in the definition itself. It is clear that this components substitute the out-of-plane related elements i and Ω.

Element set

The EI orbital element set is then composed of:

$$
\left\{ \begin{array}{llll} a & \equiv & \text{Semimajor axis} & [L] \\ e_x = e \cos \omega & \equiv & \text{x-projection of } \underline{e} & [--] \\ e_y = e \sin \omega & \equiv & \text{y-projection of } \underline{e} & [--] \\ i_x & \equiv & \text{x-component of } \underline{i} & [--] \\ i_y & \equiv & \text{y-component of } \underline{i} & [--] \\ \lambda = \omega + M & \equiv & \text{Mean argument of latitude} & [rad] \end{array} \right. \tag{A.4}
$$

A.2.2.3 Quasi-nonsingular orbital elements (QNSOE).

The quasi-nonsingular (QNS) orbital element set tackles the singularity existing in circular orbits [9], [10] [11]. It is quite similar to the formerly defined EI set, as it uses again the components of the eccentricity vector to substitute e and ω. The set is then defined as:

$$
\begin{cases}
a & \equiv \text{ Semimajor axis} & [L] \\
q_1 = e \cos\omega & \equiv \text{ x-projection of } \underline{e} & [--] \\
q_2 = e \sin\omega & \equiv \text{ y-projection of } \underline{e} & [--] \\
i & \equiv \text{ Inclination} & [rad] \\
\Omega & \equiv \text{ Right ascension of the ascending node} & [rad] \\
u = \omega + \theta & \equiv \text{ True argument of latitude} & [rad]
\end{cases}
\tag{A.5}
$$

Though some authors use a different order, this is the one used in this thesis, so as to keep the time-varying element on the last place.

A.2.2.4 Equinoctial orbital elements (EOE).

The QNS set of elements only solved half of the singularity problem. To solve both, thus enabling the description of equatorial and polar orbits, the equinoctial set of elements is defined as:

$$
\begin{cases}
a & \equiv \text{ Semimajor axis} & [L] \\
P_1 = e \cos\varpi & \equiv \textit{ unclear physical meaning, similar to } e_x & [--] \\
P_2 = e \sin\varpi & \equiv \textit{ unclear physical meaning, similar to } e_y & [--] \\
Q_1 = \tan\frac{i}{2}\cos\Omega & \equiv \textit{ unclear physical meaning, similar to } i_x & [--] \\
Q_2 = \tan\frac{i}{2}\sin\Omega & \equiv \textit{ unclear physical meaning, similar to } i_y & [--] \\
L = \Omega + \omega + \theta & \equiv \text{ True longitude} & [rad]
\end{cases}
\tag{A.6}
$$

Not only does the order does change depending on the author, but also the symbols to refer to them. An example of its use is [9].

A.2.2.5 Delaunay orbital elements (DOE).

Delaunay elements arise when formulating the two-body problem through analytical mechanics. All of the previous element sets are clearly non-canonical (*i.e.* they do not satisfy Hamilton's equations). Starting from the canonical set of elements (see appendix **??**), Delaunay elements are reached

after performing a canonical transformation, leading to the following definition:

$$
\begin{cases}
L = \sqrt{\mu\, a} & \equiv & unclear\ physical\ meaning & [L^{1/2}] \\
G = L\sqrt{1 - e^2} & \equiv & \text{Angular momentum} & [L^{1/2}] \\
H = G\cos i & \equiv & \text{Polar component of angular momentum} & [L^{1/2}] \\
l = M & \equiv & \text{Mean anomaly} & [rad] \\
g = \omega & \equiv & \text{Argument of perigee} & [rad] \\
h = \Omega & \equiv & \text{Right ascension of ascending node} & [rad]
\end{cases}
\tag{A.7}
$$

This set is mainly used in the context of perturbations, as it yields a very convenient expression for the perturbed Hamiltonian (see section **PUT SECTION HERE**).

A.3   Relative sets.

Relative elements are at the deepest roots of spacecraft relative motion, offering several advantages over cartesian relative states. First and foremost, they are more intuitive, but they also lead to a reduction of linearisation errors when expanding the deputy's movement around the chief's orbit [12]. In general, relative elements are defined as:

$$
\delta\underline{OE} = \boldsymbol{f}\left(\underline{OE_C}, \underline{OE_D}\right)
\tag{A.8}
$$

which is usually simplified by just taking the arithmetic difference between them, namely

$$
\delta\underline{OE} = \underline{OE_D} - \underline{OE_C}
\tag{A.9}
$$

where the subscripts denote respectively the deputy and chief spacecraft. The question now is, how do transformations between ROEs work.

A.3.1   Workflow for transformations between ROEs.

As for the absolute elements, Keplerian elements will be used as a pivot point. That means that only the transformations from and to RKOEs must be implemented. There are then two types of transformations:

A) From any ROE set to RKOE

While authors provide with scenarios expressed in their own ROE set, the element choice for our simulator is the Keplerian set. That leads us to the need of implementing a transformation from the former set to the latter. Let us assume then the following inputs and outputs:

- **Inputs**:

  - $\widetilde{\underline{ROE}} = \delta\widetilde{\underline{OE}}$: Different type of ROEs, whose absolute equivalents are known as a function of the KOEs ($\widetilde{\underline{OE}} = \boldsymbol{f}\left(\underline{KOE}\right)$)

  - $\underline{KOE_C}$: Chief spacecraft/reference orbit KOEs

- **Output**:

  - $\underline{RKOE} = \delta\underline{KOE}$: Keplerian ROEs

Taking equation (**??**) and particularizing it for KOEs:

$$\delta\underline{KOE} = \underline{KOE_D} - \underline{KOE_C} \tag{A.10}$$

while the second term is known (input), the second one must be calculated through a certain process:

1. Calculate chief's OEs in the source phase space (*i.e.* $\widetilde{\underline{OE}}_C$)

$$\widetilde{\underline{OE}}_C = \boldsymbol{G}_{KOE\to\widetilde{OE}}\left(\underline{KOE_C}\right)$$

2. Compute deputy's OEs by direct addition

$$\widetilde{\underline{OE}}_D = \widetilde{\underline{OE}}_C + \delta\widetilde{\underline{OE}}$$

3. Compute deputy's KOEs by back-transformation

$$\underline{KOE_D} = \boldsymbol{G}_{\widetilde{OE}\to KOE}\left(\underline{OE_D}\right)$$

4. Subtract chief's KOEs from deputy's

$$\delta\underline{KOE} = \underline{KOE_D} - \underline{KOE_C}$$

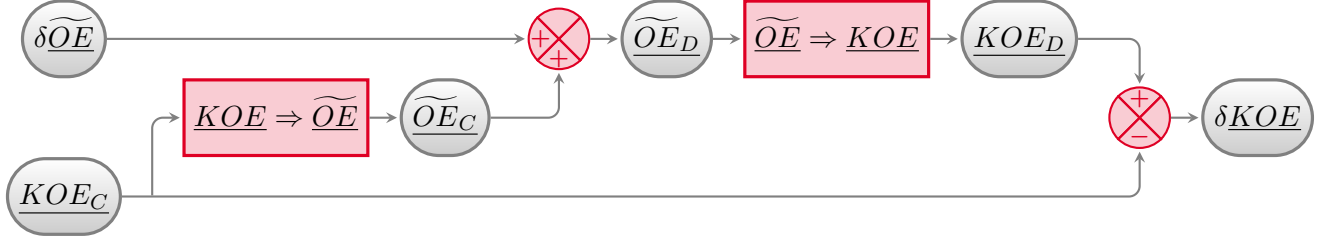See graphic **??** for a more visual explanation.

Figure A.3: Workflow for transforming any relative set into KOE.

B) From RKOE to any ROE set

In this case, let us assume the next inputs and outputs:

- **Inputs:**

  - $\underline{RKOE} = \delta\underline{KOE}$: Keplerian ROEs

  - $\underline{KOE_C}$: Chief KOEs

- **Output**:

  - $\widetilde{\underline{ROE}} = \delta\widetilde{\underline{OE}}$: Different type of ROEs, whose absolute equivalents are known as a function of the KOEs ($\widetilde{\underline{OE}} = \underline{f}(\underline{KOE})$)

For this transformation, the equation **??** particularized for this case acquires the following shape:

$$\delta\widetilde{\underline{OE}} = \widetilde{\underline{OE_D}} - \widetilde{\underline{OE_C}} \tag{A.11}$$

Equation **??** can be tackled in two main ways:

A. Using the pertinent transformations, compute the absolute elements for both spacecrafts $\widetilde{\underline{OE_D}}$, $\widetilde{\underline{OE_C}}$, and then calculate the arithmetic difference (in a **??**). See graphic **??**.

B. Expand the deputy absolute OEs (*i.e.* $\widetilde{\underline{OE_D}}$) around the chief via a Taylor series expansion with respect to the Keplerian set of elements, retaining terms up to first order, achieving a linearised expression for the transformation. Mathematically:

$$\widetilde{\underline{OE_D}} = \widetilde{\underline{OE}}(\underline{KOE_D}) = \widetilde{\underline{OE}}(\underline{KOE_C} + \delta\underline{KOE})) = \widetilde{\underline{OE_C}} + \frac{\partial\widetilde{\underline{OE}}}{\partial\underline{KOE}}\delta\underline{KOE} + \mathcal{O}\left(\delta\underline{KOE}^2\right)$$
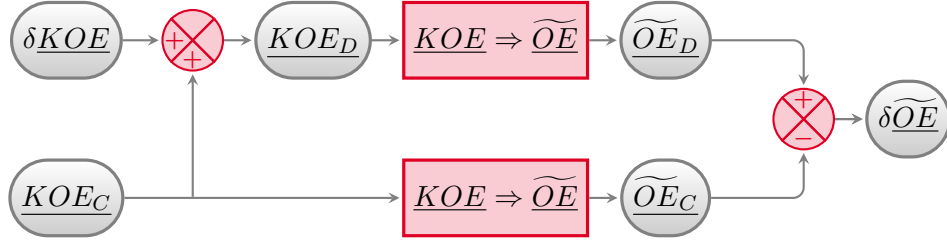
Figure A.4: Workflow for transforming RKOE into any other set.

hence,

$$\delta\widetilde{\underline{OE}} \approx \widetilde{\underline{OE_C}} + \frac{\partial\widetilde{\underline{OE}}}{\partial\underline{KOE}}\delta\underline{KOE} - \widetilde{\underline{OE_C}} = \frac{\partial\widetilde{\underline{OE}}}{\partial\underline{KOE}}\delta\underline{KOE} \qquad (A.12)$$

where the Jacobian matrix is generally simple, as it usually only implies polynomic or trigonometric functions. Equation (??) is then a first order approximation of (??). Its validity is then reduced to a close proximity between both spacecrafts, which should be assessed.

A.3.2   Element sets.

Besides the ones derived directly from its absolute counterparts, a couple of additional ROE sets will be herewith defined and explained. This is due to one of two reasons. The first one is that some ROE sets are only defined in relative terms, lacking any absolute equivalent. The second one is that it might be interesting to dive in the meaning of the relative sets, deriving interesting relations that would otherwise be overlooked.

A.3.2.1   Relative eccentricity/inclination vectors orbital elements (REIOE).

This ROE set is the counterpart of the EI set (see **??**). It is nonetheless interesting to see the meaning and shape of it, as it is quite widely used in literature [8, 10, 11]. Let us first define its elements, to later analyze the meaning behind them:

$$\begin{cases} \delta a & \equiv \quad \text{Relative semimajor axis} & [L] \\ \delta e_x & \equiv \quad \text{Relative x-component of } \underline{e} & [--] \\ \delta e_y & \equiv \quad \text{Relative y-component of } \underline{e} & [--] \\ \delta i_x & \equiv \quad \text{Relative x-component of } \underline{i} & [--] \\ \delta i_y & \equiv \quad \text{Relative y-component of } \underline{i} & [--] \\ \delta\lambda & \equiv \quad \text{Relative mean argument of latitude} & [rad] \end{cases} \qquad (A.13)$$
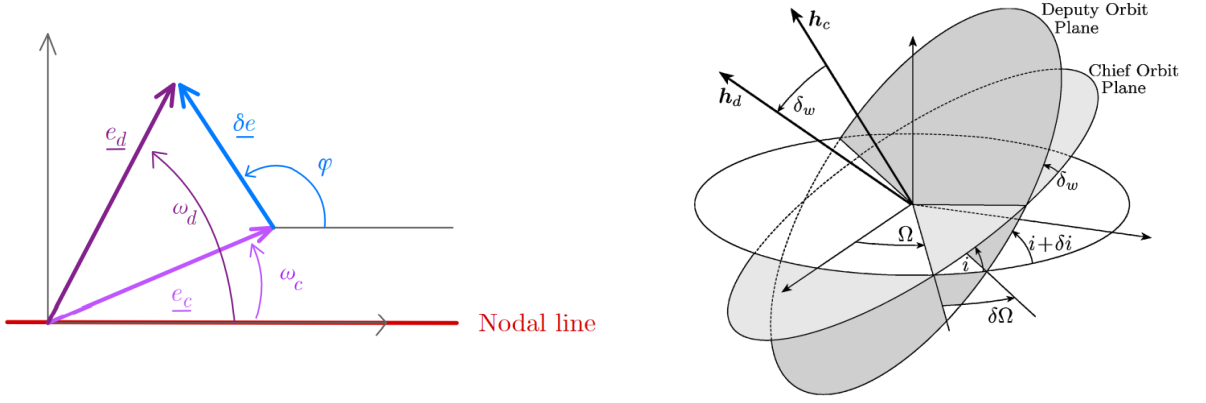
(a) Relative eccentricity vector.

(b) Relative inclination vector [11] .

Figure A.5: Relative ccentricity & inclination vectors.

Concept & meaning

The relative eccentricity vector components substitute the relative eccentricity and the relative argument of perigee. It is based on the eccentricity vector definition (**??**), and a graphical representation can be seen in figure **??**. Mathematically:

$$
\delta \underline{e} = \left\{ \begin{array}{c} \delta e_x \\ \\ \delta e_y \end{array} \right\} = \delta e \left\{ \begin{array}{c} \cos \varphi \\ \\ \sin \varphi \end{array} \right\}
$$

which rules the in-plane relative motion (hand in hand with δa and $\delta \lambda$). As we know, there are two ways of tackling the transformation from RKOE to this set (see **??**). Though the nonlinear form is exact, let us analyze the linear version. If we assume that the difference in the eccentricity vector is due to that of the eccentricity and argument of perigee (δe, $\delta \omega$), we arrive to:

$$
\delta \underline{e} \approx \left[\begin{array}{cc} \cos \omega & -e \sin \omega \\ \\ \sin \omega & e \cos \omega \end{array} \right] \left\{ \begin{array}{c} \delta e \\ \\ \delta \omega \end{array} \right\} \tag{A.14}
$$

where we have neglected terms of second order and higher. The relative inclination vector is defined in an alternative way [8] (comparing with the absolute counterpart). Mathematically:

$$\delta\underline{i} = \sin\delta i \left\{ \begin{array}{c} \cos\theta \\ \\ \sin\theta \end{array} \right\}$$

where θ is the analog angle to φ in the eccentricity vector. Once again, let us analyze the linearized transformation from RKOE to this set, considering the differences δi and $\delta\Omega$. Applying the law of sines and the law of cosines for spherical trigonometry and assuming small values of δi and $\delta\Omega$, we arrive to:

$$\delta\underline{i} = \left\{ \begin{array}{c} \delta i \\ \\ \sin i \delta\Omega \end{array} \right\} \approx \left[\begin{array}{cc} 1 & 0 \\ \\ 0 & \sin i \end{array} \right] \left\{ \begin{array}{c} \delta i \\ \\ \delta\Omega \end{array} \right\} \tag{A.15}$$

where i is the inclination of the chief's orbit. Combining the results of (**??**) and (**??**) with the definitions of the remaining elements, we can easily arrive to an expression analog to (**??**):

$$\left\{ \begin{array}{c} \delta a \\ \delta e_x \\ \delta e_y \\ \delta i_x \\ \delta i_y \\ \delta\lambda \end{array} \right\} \approx \left[\begin{array}{cccccc} 1 & 0 & 0 & 0 & 0 & 0 \\ 0 & \cos\omega & 0 & 0 & -e\sin\omega & 0 \\ 0 & \sin\omega & 0 & 0 & e\cos\omega & 0 \\ 0 & 0 & 1 & 0 & 0 & 0 \\ 0 & 0 & 0 & \sin i & 0 & 0 \\ 0 & 0 & 0 & 0 & 1 & 1 \end{array} \right] \left\{ \begin{array}{c} \delta a \\ \delta e \\ \delta i \\ \delta\Omega \\ \delta\omega \\ \delta M \end{array} \right\} \tag{A.16}$$

A graphical representation of this concept can be seen in figure **??**.

A.3.2.2   Peters-Noomen C set of relative orbital elements (CROE).

Defined by Peters & Noomen in [5], this set is also closely related with the orbit safety notion. It arises from the analysis of the Gauss Variational Equations (GVEs) applied to the relative dynamics between a deputy and a chief spacecraft, when the former performs a cotangential transfer. Without

further ado, let us define them as:

$$
\begin{cases}
C_1 = \delta p = \eta^2 \delta a - 2\,a\,e\delta e & \equiv & \text{Relative parameter of the orbit} & [L] \\[2mm]
C_2 = e\delta p - p\delta e & \equiv & \textit{unclear physical meaning} & [L] \\[2mm]
C_3 = -e\,p\,(\delta\omega + \cos i\delta\Omega) & \equiv & \textit{unclear physical meaning} & [L] \\[2mm]
C_4 = a\,(\delta\omega + \cos i\delta\Omega + \eta^{-1}\delta M) & \equiv & \text{Modified relative mean longitude} & [L] \\[2mm]
C_5 = -p\,(\cos\omega\delta i + \sin i \sin\omega\delta\Omega) & \equiv & \textit{unclear physical meaning} & [L] \\[2mm]
C_6 = p\,(\sin\omega\delta i - \sin i \cos\omega\delta\Omega) & \equiv & \textit{unclear physical meaning} & [L]
\end{cases}
\tag{A.17}
$$

For a proper geometrical and conceptual description of the elements, please see [5]. As an introduction, the first four elements essentially determine the in-plane relative motion. C_1, C_2 & C_3 arise from a very intelligent interpretation of the GVEs, with C_4 completing the element set. On the other hand, elements C_5 and C_6 describe the out-of-plane motion.

Cartesian reference systems.

B.1 Introduction.

Cartesian states are, as mentioned in appendix **??**, one of the two main alternatives to describe the state of a certain spacecraft (or celestial body). Though orbital elements (OEs) are generally more intuitive and meaningful, these states are quite critical for the description of both absolute and relative motion. Ultimately, and specially considering the latter, we wish to know the relative orientation and linear distance between the involved bodies. During this appendix, a set of absolute and relative reference frames will be described and related via transformations, which have been used time and again along this thesis.

B.1.1 Inertial and rotating reference frames.

Technically, an inertial reference frame is one where Newton's law holds. Effectively, it is a frame which is not object of any acceleration whatsoever. It is then, when interpreted to the letter, an idealization, as there will always be any perturbation which disavows this assumption. Nonetheless, it is usual to neglect said perturbations up to a certain point, thus considering pseudo-inertial reference frames. From now on then, when inertial reference frames are mentioned they will be considered so, even though they are actually not. Along this thesis, both inertial and rotating frames will be considered, each bearing its different advantages and disadvantages.

B.1.2 Absolute and relative frames.

Another distinction that will be made is between absolute and relative frames. In this thesis, absolute frames are those who are centered in the Earth's center of mass, while relative frames are defined with respect to a reference orbit (the chief's generally). Again, they have different scopes, though relations between them need to be developed.

B.1.3 Time measurement.

Later it will be described how Earth's rotational state influences the dynamics of the spacecrafts, due to its non-homogeneous mass distribution. That leads to the need of precisely computing it,

which in turn requires the time elapsed since a given epoch. This section intends to briefly describe the most usual conventions for time definition, without diving in technical considerations. For further description, see [13]. These conventions are:

I. <u>International Atomic Time</u> (TAI): Physical timescale which is calculated through the measurement of cesium radiation. Lacks intuitive meaning, but acts as a ultra-high precision time system and reference for other timescales.

II. <u>Universal Time</u> (UT1/UT2): Civil time system, which is defined by the right ascension of the mean Sun. It is not a continuous time system, varying as time passes.

III. <u>Coordinated Universal Time</u> (UTC): Civil time system, which is measured with TAI and synchronized with UT1 via leap seconds to get within 1-second range. It is then a non-continuous time system.

IV. <u>Terrestrial Time</u> (TT): Civil time system, which is measured with TAI but has a delay with respect to it (32.184 seconds).

Figure **??** shows more clearly the differences between them.
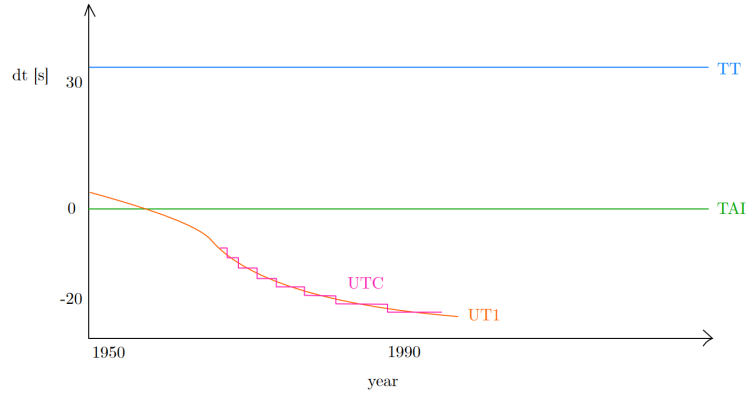

Figure B.1: Sketch of the different time systems.

B.2 Transformations between reference systems.

In this section, two approaches for reference system transformations will be presented. These will prove quite useful later on, helping to clarify how different systems relate to each other.

For the sake of generality, let us consider an inertial and absolute reference frame, and a rotating, relative reference frame (see figure **??**). In case we need to consider two absolute systems, it is enough to just nullify the displacement between both frames' origins. The notation used is described below:

- <u>Vectors</u>: $\underline{X}$ refers to a vector with respect an absolute frame, while $\underline{x}$ is used for relative reference frames. Please, note that we are not making use of any reference system (*i.e.* vector base): we are just considering the vector entity as an object.

- <u>Subscripts</u>: Unless specified otherwise, denote the body: $\bullet_C$ for the chief, $\bullet_D$ for the deputy.

- <u>Time derivatives and superscripts</u>: As Coriolis' Theorem states, when non-inertial reference frames are involved, it is necessary to specify the frame with respect to which the derivative is calculated. $\dfrac{^\mathcal{F}d\bullet}{dt}$ denotes the time derivative in the frame $\mathcal{F}$. An equally valid yet more compact notation is $\dot{\bullet}^\mathcal{F}$.

- <u>Right vertical bar subscript</u>: Denotes the coordinate system in which one vector or matrix is described. For example, $\underline{u}|_1 = \sum_{i=1}^{3} u_{xi}\underline{\hat{e}_{i1}}$.
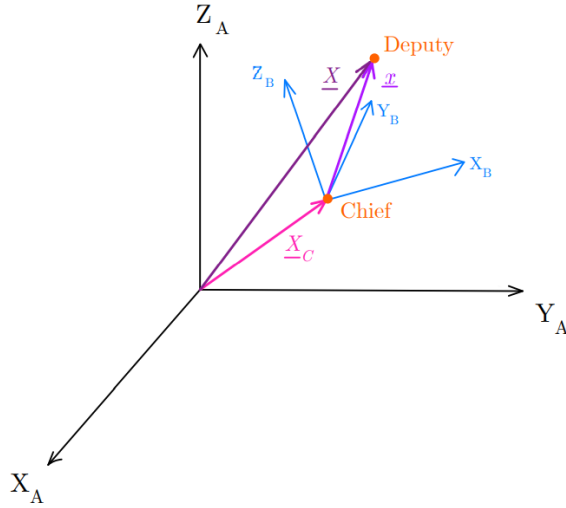

Figure B.2: Absolute and relative frames.

Consider the frames A and B from figure **??**. Let us address firstly the transformation from $A \rightarrow B$, that is, converting an absolute & inertial state vector expressed in coordinate system A to the relative, rotating frame B in its coordinates. What we would like to achieve is a relationship of the form:

$$\begin{cases} \underline{x}|_B &= \boldsymbol{f}_1\left(\underline{X}|_A, ---, \underline{X_C}|_A, ---\right) \\ \underline{\dot{x}}^B|_B &= \boldsymbol{f}_2\left(\underline{X}|_A, \underline{\dot{X}}^A|_A, \underline{X_C}|_A, \underline{\dot{X_C}}^A|_A\right) \end{cases}$$

As it turns out, this relation is actually linear on the inputs $\underline{\dot{X}}^A|_A$ and $\underline{X}|_A$. From this point on, two approaches are derived:

B.2.1   Direct analytical differentiation.

The first approach starts from the decomposition of the deputy's absolute position vector [14]:

$$\underline{X} = \underline{X_C} + \underline{x} \rightarrow \underline{x} = \underline{X} - \underline{X_C}$$

This vector can be expressed in both coordinate systems, namely $\underline{x}|_A$ and $\underline{x}|_B$. The transformation between them can be written as the following rotation:

$$\underline{x}|_B = R_{A \rightarrow B} \underline{x}|_A \tag{B.1}$$

The rotation matrix $R_{A \rightarrow B}$ takes the following form:

$$R_{A \rightarrow B} = \begin{bmatrix} \left(\hat{e}_{xA} \cdot \hat{e}_{xB}\right) & \left(\hat{e}_{yA} \cdot \hat{e}_{xB}\right) & \left(\hat{e}_{zA} \cdot \hat{e}_{xB}\right) \\ \left(\hat{e}_{xA} \cdot \hat{e}_{yB}\right) & \left(\hat{e}_{yA} \cdot \hat{e}_{yB}\right) & \left(\hat{e}_{zA} \cdot \hat{e}_{yB}\right) \\ \left(\hat{e}_{xA} \cdot \hat{e}_{zB}\right) & \left(\hat{e}_{yA} \cdot \hat{e}_{zB}\right) & \left(\hat{e}_{zA} \cdot \hat{e}_{zB}\right) \end{bmatrix}$$

where each column is the coordinates of each base vector of the "origin" coordinate system expressed in the "final" one. This fact is specially useful when such vectors are characteristic of the problem at hand, as it is the case for the two body problem. In order to transform the velocity vector, let us just take the time derivative of **??**, yielding:

$$\underline{\dot{x}}|_B = \dot{R}_{A \rightarrow B} \underline{x}|_A + R_{A \rightarrow B} \underline{\dot{x}}|_A \tag{B.2}$$

whose first derivative $\dot{R}_{A \rightarrow B}$ can be calculated by columns, simplifying the task at hand if we have been able to obtain the origin base $\left(\hat{e}_{xA}, \hat{e}_{yA}, \hat{e}_{zA}\right)$ in terms of the final one. For the sake of completeness, let us remind that [14]:

$$\frac{d}{dt}\hat{\underline{u}} = \frac{1}{u}\left[\underline{\dot{u}} - \left(\hat{\underline{u}} \cdot \underline{\dot{u}}\right)\hat{\underline{u}}\right] \tag{B.3}$$

A final, more compact form of both **??** and **??** can be reached by rearranging terms:

$$\left\{\begin{array}{c} \underline{x}|_B \\ \underline{\dot{x}}^B|_B \end{array}\right\} = \left[\begin{array}{cc} R_{A \rightarrow B} & 0_{3x3} \\ \dot{R}_{A \rightarrow B} & R_{A \rightarrow B} \end{array}\right] \left\{\begin{array}{c} \underline{X}|_A - \underline{X_C}|_A \\ \underline{\dot{X}}^A|_A - \underline{\dot{X}_C}^A|_A \end{array}\right\} \tag{B.4}$$

and the inverse transformation can be expressed as:

$$
\left\{ \begin{array}{c} \underline{X}|_A \\ \underline{\dot{X}}^A|_A \end{array} \right\} = \left[\begin{array}{cc} R_{B\to A} & 0_{3x3} \\ \dot{R}_{B\to A} & R_{B\to A} \end{array} \right] \left\{ \begin{array}{c} \underline{x}|_B \\ \underline{\dot{x}}^B|_B \end{array} \right\} + \left\{ \begin{array}{c} \underline{X_C}|_A \\ \underline{\dot{X}_C}^A|_A \end{array} \right\}
\tag{B.5}
$$

An example of this approach will be developed later on in **??**.

B.2.2 Classical motion composition.

This approach, rather on pure derivation, is based on the grounds of motion composition and Coriolis' Theorem. This theorem states that the derivative of a vector in an inertial frame is equivalent to the derivative in a rotating frame plus another contribution due to the rotation of this reference frame:

$$
\frac{^A d\underline{u}}{dt} = \frac{^B d\underline{u}}{dt} + \underline{\omega}_{B||A} \times \underline{u}
$$

The first term of the right-hand side is associated to the temporal variation of the coordinates of $\underline{u}$ in the rotating frame, whereas the second one is purely related to the relative rotation between both frames. If we apply this to **??**:

$$
\frac{^A d\underline{X}}{dt} = \frac{^A d\underline{X_C}}{dt} + \frac{^A d\underline{x}}{dt} = \frac{^A d\underline{X_C}}{dt} + \frac{^B d\underline{x}}{dt} + \underline{\omega}_{B||A} \times \underline{x}
$$

$$
\Rightarrow \underline{\dot{X}}^A = \underline{\dot{X}_C}^A + \underline{\dot{x}}^B + \underline{\omega}_{B||A} \times \underline{x}
\tag{B.6}
$$

As before, let us first go from the inertial frame towards the rotating. For that purpose, let us substitute (**??**) into (**??**), solving for $\underline{\dot{x}}^B$:

$$
\underline{\dot{x}}^B = \underline{\dot{X}}^A - \underline{\dot{X}_C}^A - \underline{\omega}_{B||A} \times \left(\underline{X} - \underline{X_C} \right)
\tag{B.7}
$$

Now, expressing every vector in its proper frame:

$$
\underline{\dot{x}}^B|_B = R_{A\to B} \left[\underline{\dot{X}}^A|_A - \underline{\dot{X}_C}^A|_A + \underline{\omega}_{A||B}|_A \times \left(\underline{X}|_A - \underline{X_C}|_A \right) \right]
\tag{B.8}
$$

Let's make use now of the axial-dual vector form, leading to:

$$
\underline{\dot{x}}^B|_B = R_{A\to B} \left[\underline{\dot{X}}^A|_A - \underline{\dot{X}_C}^A|_A + \Omega_{A||B}|_A \left(\underline{X}|_A - \underline{X_C}|_A \right) \right]
\tag{B.9}
$$

where $\Omega_{A||B}$ is the matrix dual form of $\underline{\omega}_{A \to B}$, that is:

$$\Omega_{A||B} = \begin{bmatrix} 0 & -\omega_z & \omega_y \\ \omega_z & 0 & -\omega_x \\ -\omega_y & \omega_x & 0 \end{bmatrix}$$

We can now express the conversion in a far more compact form as:

$$\left\{ \begin{array}{c} \underline{x}|_B \\ \underline{\dot{x}}^B|_B \end{array} \right\} = \begin{bmatrix} R_{A \to B} & 0_{3x3} \\ R_{A \to B}\Omega_{A||B}|_A & R_{A \to B} \end{bmatrix} \left\{ \begin{array}{c} \underline{X}|_A - \underline{X}_C|_A \\ \underline{\dot{X}}^A|_A - \underline{\dot{X}_C}^A|_A \end{array} \right\} \tag{B.10}$$

and its inverse can be easily derived, leading to:

$$\left\{ \begin{array}{c} \underline{X}|_A \\ \underline{\dot{X}}^A|_A \end{array} \right\} = \begin{bmatrix} R_{B \to A} & 0_{3x3} \\ R_{B \to A}\Omega_{B||A}|_B & R_{B \to A} \end{bmatrix} \left\{ \begin{array}{c} \underline{x}|_B \\ \underline{\dot{x}}^B|_B \end{array} \right\} + \left\{ \begin{array}{c} \underline{X}_C|_A \\ \underline{\dot{X}_C}^A|_A \end{array} \right\} \tag{B.11}$$

Comparing (**??**) and (**??**), we extract an interesting property of $\dot{R}$, namely:

$$\dot{R}_{A \to B} = R_{A \to B}\Omega_{A||B}|_A$$

which is in turn quite useful, as time derivation of the rotation matrix itself might be quite costly and symbolically dense. This requires though to know the angular velocity vector, whose calculation might not be easy.

B.3   Absolute reference systems.

B.3.1   Earth-Centered-Inertial reference system (ECI).

As previously stated, any Earth-centered reference system will in turn be non-inertial. That leads to the need of defining a common baseline, *i.e.* an epoch at which the reference system is known. The chosen epoch is denoted as J2000.0[1], which translates to January 1$^{\text{st}}$, at 12:00:00.000 (midday) in Julian years [see 13, glossary]. Effectively, the ECI reference system, is geometrically defined as

---

[1] J2000 denotes a reference frame, being analog to ECI. J2000.0 refers to the mentioned epoch.

follows [15]:

$$
ECI \equiv \begin{cases}
\text{Origin} & \equiv & \text{Earth's COM} \\[2ex]
\text{X-axis} & \equiv & \text{Earth's COM} \longrightarrow \text{Mean vernal equinox at epoch J2000.0} \\[2ex]
\text{Z-axis} & \equiv & \text{Normal to the mean equatorial plane at epoch J2000.0,} \\[1ex]
& & \text{pointing towards the Northern Hemisphere} \\[2ex]
\text{Y-axis} & \equiv & \text{Perpendicular to the X and Z axes forming a right-handed system}
\end{cases}
$$

The main reason behind using this system is that it considerably simplifies the dynamics equation of any spacecraft. It is then the most adequate frame on which dynamics can be solved. Furthermore, when considering relative motion, the reference axis are not a critical axis, as we are rather focused on the motion between spacecrafts. On the other hand, this frame is not able to describe the position relative to Earth's surface, thus being useless in communications or visibility analysis.

B.3.2   Earth-Centered, Earth-Fixed reference system (ECEF).

Due to the formerly mentioned concerns, another Earth-centered reference frame must be defined. In this case, that will be ECEF. Geometrically, it is defined as [15]

$$
ECEF \equiv \begin{cases}
\text{Origin} & \equiv & \text{Earth's COM} \\[2ex]
\text{X-axis} & \equiv & \text{Earth's COM} \longrightarrow \text{Intersection of prime meridian and true equatorial plane} \\[2ex]
\text{Z-axis} & \equiv & \text{Earth's true angular velocity vector (rotation axis)} \\[2ex]
\text{Y-axis} & \equiv & \text{Perpendicular to the X and Z axes forming a right-handed system}
\end{cases}
$$

Once defined, it is turn to evaluate how ECI and ECEF frames differ.

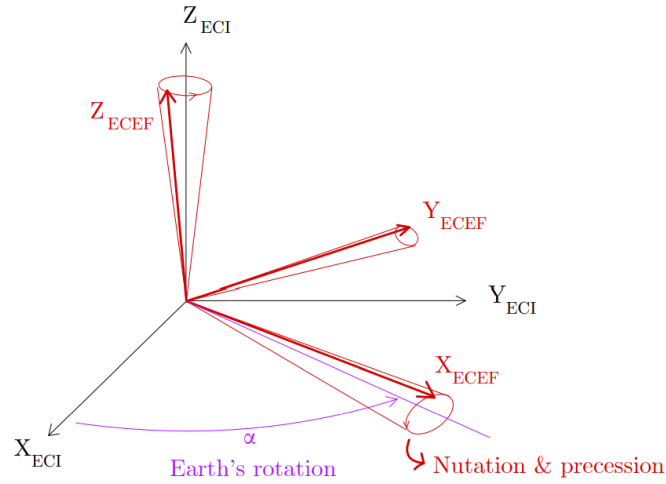### B.3.2.1   Conversion from ECI to ECEF.

Figure B.3: ECI and ECEF reference frames.

Decomposition of the conversion.

There are four essential differences between ECI and ECEF frame, due to four motions that ECEF include due to it being fixed to Earth:

1. Precession of the equinoxes.

2. Nutations (small oscillations) of the equinoxes.

3. Earth's rotation around its axis.

4. Spin axis motion.

Each of this motions can be characterized by a rotation to an associated frame. That is, we can decompose the conversion between ECI and ECEF in four rotations, which will now be analyzed.

Involved intermediate frames & rotations.

ECI(J200) to Mean of Date.

The equinoxes rotate at a slow, but relevant rate. That means that the vernal equinox today differs considerably from the one at J2000.0. The Mean of Date (MOD) frame arises from this notion, being defined as [15]:

$$
MOD \equiv
\begin{cases}
\text{X-axis} & \equiv & \text{Earth's COM} \longrightarrow \text{Mean vernal equinox at current epoch} \\
\\
\text{Z-axis} & \equiv & \text{Perpendicular to the mean equatorial plane at current epoch} \\
\\
\text{Y-axis} & \equiv & \text{Perpendicular to the X and Z axes forming a right-handed system}
\end{cases}
$$

The rotation matrix from J200 to MOD results:

$$
R_{ECI \to MOD} =
\begin{bmatrix}
C\zeta_A C\theta_A Cz_A - S\zeta_A Sz_A & -S\zeta_A C\theta_A Cz_A - C\zeta_A Sz_A & -S\theta_A Cz_A \\
C\zeta_A C\theta_A Sz_A + S\zeta_A Cz_A & -S\zeta_A C\theta_A Sz_A + C\zeta_A Cz_A & -S\theta_A Sz_A \\
C\zeta_A S\theta_A & -S\zeta_A S\theta_A & C\theta_A
\end{bmatrix}
\tag{B.12}
$$

where the precession angles ζ_A, θ_A and z_A, which are functions of the epoch, are shown in [15], page 519. S and C are abbreviations of the sine and cosine functions.
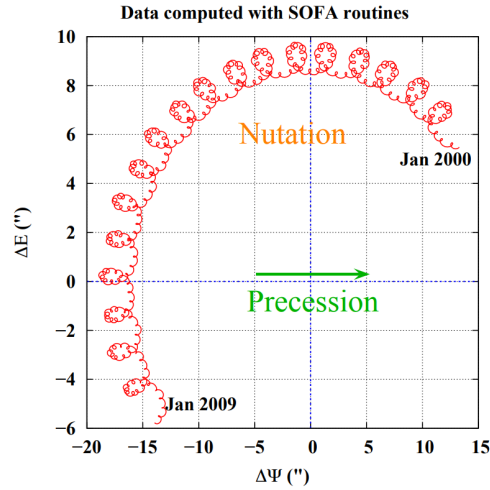

Figure B.4: Nutation and precession motion.

Mean of Date to True of Date

Besides the "long-term" precession motion, equinoxes suffer also short-period, small oscillations, which are denoted as nutations. For more clarity, see figure **??**. The True of Date (TOD) frame is thus defined as:

$$
TOD \equiv
\begin{cases}
\text{X-axis} & \equiv & \text{Earth's COM} \longrightarrow \text{True vernal equinox at current epoch} \\[2mm]
\text{Z-axis} & \equiv & \text{Perpendicular to the true equatorial plane at current epoch} \\[2mm]
\text{Y-axis} & \equiv & \text{Perpendicular to the X and Z axes forming a right-handed system}
\end{cases}
$$

The rotation matrix now has the following shape:

$$
R_{MOD \to TOD} =
\begin{bmatrix}
C\Delta\psi & -C\epsilon_m S\Delta\psi & -S\epsilon_m S\Delta\psi \\
C\epsilon_t S\Delta\psi & C\epsilon_m C\epsilon_t C\Delta\psi + S\epsilon_m S\epsilon_t & S\epsilon_m C\epsilon_t C\Delta\psi - C\epsilon_m S\epsilon_t \\
S\epsilon_t S\Delta\psi & C\epsilon_m S\epsilon_t C\Delta\psi - S\epsilon_m C\epsilon_t & S\epsilon_m S\epsilon_t C\Delta\psi + C\epsilon_m C\epsilon_t
\end{bmatrix}
\tag{B.13}
$$

where four angles appear. Firstly, the mean obliquity, which is the angle between the mean ecliptic and the mean equatorial plane ($\approx 23.5°$). For an analytic expression, see [15], page 519. Moreover, two nutations arise: one in longitude and one in obliquity ($\Delta\psi$ and $\Delta\epsilon$, respectively). This angles are computed by a summation of a large number of sinusoidal functions, whose construction and coefficients are shown in [16]. Lastly, the true obliquity is simply the addition of its mean counterpart and the nutation ($\epsilon_t = \epsilon_m + \Delta\epsilon$).

True of Date to Pseudo-Body-Fixed

Perhaps the biggest and most intuitive difference between ECI and ECEF is Earth's rotation around its axis. The pseudo-body-fixed is simply a clockwise rotation (seen from north pole towards the Earth's COM) around said axis from the True of Date frame:

$$
PBF \equiv
\begin{cases}
\text{X-axis} & \equiv & \text{Earth's COM} \longrightarrow \text{Intersection between prime meridian and true equatorial plane} \\
& & \text{(without accounting for the axis' displacement).} \\[2mm]
\text{Z-axis} & \equiv & \text{Perpendicular to the true equatorial plane at current epoch} \\[2mm]
\text{Y-axis} & \equiv & \text{Perpendicular to the X and Z axes forming a right-handed system}
\end{cases}
$$

The rotation matrix is now as simple as:

$$
R_{TOD \to PBF} =
\begin{bmatrix}
C\alpha_G & S\alpha_G & 0 \\
-S\alpha_G & C\alpha_G & 0 \\
0 & 0 & 1
\end{bmatrix}
\tag{B.14}
$$

where α_G is referred to as the Greenwich Mean Sidereal Time (GMST). $\dot{\alpha}_G$ is then the rotation rate of the Earth. An analytical expression for this angle is provided in [15], page 520 (eq. H.4.3).

Pseudo-Body-Fixed to Body-Fixed (ECEF)

The last, and surely most subtle transformation, is the one that accounts for the displacement in Earth's axis of rotation. This displacement is parametrized with the polar angles x_p and y_p, which can again be found at [16]. As these angles are sufficiently small, the rotation matrix from PBF to ECEF is:

$$R_{PBF \to BF} = \begin{bmatrix} 1 & 0 & x_p \\ 0 & 1 & -y_p \\ -x_p & y_p & 1 \end{bmatrix} \tag{B.15}$$

Full rotation matrix $R_{ECI \to ECEF}$.

By simply successively composing rotations, the full rotation matrix from ECI to ECEF is computed as:

$$R_{ECI \to ECEF} = R_{PBF \to ECEF} R_{TOD \to PBF} R_{MOD \to TOD} R_{ECI \to MOD}$$

B.3.3 Perifocal (PQW) reference frame.

B.3.3.1 Definition.

The perifocal reference frame is defined as:

$$PQW \equiv \begin{cases} \text{Origin} & \equiv & \text{Central body's COM} \\ \text{X-axis} & \equiv & \text{Origin} \longrightarrow \text{Periapsis.} \\ \text{Z-axis} & \equiv & \text{Perpendicular to the osculating orbital plane (out-of-plane)} \\ \text{Y-axis} & \equiv & \text{Perpendicular to the X and Z axes forming a right-handed system} \end{cases}$$

This frame takes advantage of the motion being contained in the orbital plane (when using osculating elements, see **CITE MEAN2OSC**). That means that usually, the problem reduces to evaluating two components of the position and velocity. It also allows for a quite straightforward description of the motion in terms of the Keplerian OEs, assuming elliptical motion. In this case, and

using $\underline{q}$ and $\underline{\dot{q}}$ to denote perifocal position and velocity, the perifocal state vector is expressed as:

$$\underline{q} = \left\{ \begin{array}{c} r\cos\theta \\ r\sin\theta \\ 0 \end{array} \right\} = \left\{ \begin{array}{c} a\left(\cos E - e\right) \\ a\sin E \\ 0 \end{array} \right\} \qquad \underline{\dot{q}} = \frac{na}{\sqrt{1 - e^2}} \left\{ \begin{array}{c} -\sin\theta \\ e + \cos\theta \\ 0 \end{array} \right\}$$

where E is the eccentric anomaly, r is the orbital radius, n is the mean orbital rate and the remaining parameters are the regular Keplerian OEs. r and n can be expressed as a function of them as:

$$r = \frac{a(1 - e^2)}{1 + e\cos\theta} = a(1 - e\cos E) \;; \qquad n = \sqrt{\frac{\mu}{a^3}}$$

with $\mu = GM$ being the gravitational parameter of the central body.

B.3.3.2   State vector transformation.

Our target is to get an expression analogous to (**??**). As both frames are Earth-centered, $\underline{X}_C = 0$, so that only the rotation and angular velocity matrices are to be found.

Rotation matrix from & to ECI.

As done with the ECI to ECEF transformation, this one can also be decomposed in three rotations, each associated with one Keplerian angle.

The first rotation is associated to Ω, being done around the Z ECI axis. The resulting frame will be named I1 (intermediate 1), and the rotation matrix from ECI is:

$$R_{ECI \to I1}(\Omega) = \begin{bmatrix} \cos\Omega & \sin\Omega & 0 \\ -\sin\Omega & \cos\Omega & 0 \\ 0 & 0 & 1 \end{bmatrix}$$

Afterwards, a rotation around X axis of I1 (nodal line) of value i is performed, leading to frame I2. The rotation matrix is simply:

$$R_{I1 \to I2}(\Omega) = \begin{bmatrix} 1 & 0 & 0 \\ 0 & \cos i & \sin i \\ 0 & -\sin i & \cos i \end{bmatrix}$$

Finally, a rotation around Z axis of I2 (out-of-plane direction) of value ω is done, yielding the desired perifocal frame (which we will denote as PQW):

$$R_{I2 \to PQW}(\Omega) = \begin{bmatrix} \cos\omega & \sin\omega & 0 \\ -\sin\omega & \cos\omega & 0 \\ 0 & 0 & 1 \end{bmatrix}$$

By composition, the matrix $R_{ECI \to PQW}$ can easily be calculated:

$$R_{ECI \to PQW} = R_{I2 \to PQW} R_{I1 \to I2} R_{ECI \to I1} = \begin{bmatrix} C\Omega C\omega - S\Omega CiS\omega & S\Omega C\omega + C\Omega CiS\omega & SiS\omega \\ -C\Omega S\omega - S\Omega Cic\omega & C\Omega CiC\omega + S\Omega S\omega & SiC\omega \\ S\Omega Si & -C\Omega Si & Ci \end{bmatrix}$$

Angular velocity.

In order to fully transform the system, it is necessary to calculate the relative angular velocity between both frames. Again, that can be done by composing the angular movements:

$$\underline{\omega}_{PQW||ECI} = \dot{\Omega}\underline{\hat{k}_{I1}} + \dot{i}\underline{\hat{i}_{I2}} + \dot{\omega}\underline{\hat{k}_{PQW}}$$

Expressing everything in PQW frame:

$$\underline{\omega}_{PQW||ECI}|_{PQW} = \begin{Bmatrix} \omega_x \\ \omega_y \\ \omega_z \end{Bmatrix} = \dot{\Omega}R_{ECI \to PQW} \begin{Bmatrix} 0 \\ 0 \\ 1 \end{Bmatrix} + \dot{i}R_{I2 \to PQW} R_{I1 \to I2} \begin{Bmatrix} 1 \\ 0 \\ 0 \end{Bmatrix} + \dot{\omega}R_{I2 \to PQW} \begin{Bmatrix} 0 \\ 0 \\ 1 \end{Bmatrix}$$

In virtue of the axial dual form principle, there exists one matrix that, when applied to a certain vector, yields the same result as doing the cross product between $\underline{\omega}$ and that vector. This matrix has the following shape:

$$\Omega_{PQW||ECI}|_{PQW} = \begin{bmatrix} 0 & -\omega_z & \omega_y \\ \omega_z & 0 & -\omega_x \\ -\omega_y & \omega_x & 0 \end{bmatrix}$$

Transformation matrices $\boldsymbol{T}_{PQW \to ECI}$, $\boldsymbol{T}_{ECI \to PQW}$.

The transformation matrices can easily be built as in (**??**):

$$
T_{PQW \to ECI} = \begin{bmatrix} R_{PQW \to ECI} & 0_{3x3} \\ R_{PQW \to ECI} \Omega_{PQW \| ECI | PQW} & R_{PQW \to ECI} \end{bmatrix}
$$

whose inverse counterpart can be obtained in terms of the same components, as:

$$
T_{ECI \to PQW} = \begin{bmatrix} R_{PQW \to ECI}^{T} & 0_{3x3} \\ -\Omega_{PQW \| ECI | PQW} R_{PQW \to ECI}^{T} & R_{PQW \to ECI}^{T} \end{bmatrix}
$$

It is important to note that, as the rotation angles are Keplerian OEs, the unperturbed assumption leads to a null angular velocity (as the orbital plane remains unchanged along time). That greatly simplifies the transformation, turning into a trivial rotation of the position and velocity vectors.

B.4 Relative reference systems.

It is time now to address relative reference frames. For each of them, a description is provided, followed by a conversion to and from the ECI reference frame.

B.4.1 RTN reference frame.

B.4.1.1 Definition.

The Radial-Tangential-Normal (RTN) reference frame is defined as [10]:

$$
RTN \equiv \begin{cases} \text{Origin} & \equiv \quad \text{Chief SC COM} \\ \text{X-axis}(\underline{e}_R) & \equiv \quad \text{Radial direction (positive outwards)} \\ \text{Z-axis}(\underline{e}_N) & \equiv \quad \text{Normal to the orbit plane (positive with orbit momentum)} \\ \text{Y-axis}(\underline{e}_T) & \equiv \quad \text{Perpendicular to the X and Z axes forming a right-handed system} \\ & \quad\quad (\approx \text{ tangent to the trajectory}) \end{cases}
$$

A graphical representation of this frame is shown in figure **??**.

Figure B.5: RTN frame [10].

B.4.1.2 State vector transformation.

As before, we need to build two matrices: The rotation matrix and the angular velocity matrix.

Rotation matrix from ECI.

If we pay close attention to both PQW and RTN frames, it arises that the rotation matrix is virtually the same, only changing the value of the last rotation from ω to $u = \theta + \omega$. That is:

$$R_{I2 \to RTN} = R_{I2 \to RTN}|_{\omega \to u} \Rightarrow R_{ECI \to RTN} = R_{ECI \to PQW}|_{\omega \to u}$$

which leads to the following expression:

$$R_{ECI \to RTN} = \begin{bmatrix} C\Omega Cu - S\Omega CiSu & S\Omega Cu + C\Omega CiSu & SiSu \\ -C\Omega Su - S\Omega CiCu & -S\Omega Su + C\Omega CiCu & SiCu \\ S\Omega Si & -C\Omega Si & Ci \end{bmatrix}$$

Angular velocity.

Assuming unperturbed motion, the only time-varying angle is u through the true anomaly. Its rate is in fact:

$$\dot{\theta} = \dot{M}\frac{\rho^2}{\eta^3} = \frac{n\rho^2}{\eta^3}$$

where $\rho = 1 + e\cos\theta$ and $\eta = \sqrt{1 - e^2}$. With this in mind, the angular velocity matrix takes the following form:

$$\Omega_{RTN||ECI}|_{RTN} = \begin{bmatrix} 0 & -\dot{\theta} & 0 \\ \dot{\theta} & 0 & 0 \\ 0 & 0 & 0 \end{bmatrix}$$

Transformation matrices $\boldsymbol{T}_{RTN \to ECI}$, $\boldsymbol{T}_{ECI \to RTN}$.

The transformation matrices are composed as follows:

$$T_{ECI \to RTN} = \begin{bmatrix} R_{ECI \to RTN} & 0_{3x3} \\ -\Omega_{RTN||ECI}|_{RTN} R_{ECI \to RTN} & R_{ECI \to RTN} \end{bmatrix}$$

whose inverse counterpart can be obtained in terms of the same components, as:

$$T_{RTN \to ECI} = \begin{bmatrix} R^T_{ECI \to RTN} & 0_{3x3} \\ R^T_{ECI \to RTN}\Omega_{RTN||ECI}|_{RTN} & R^T_{ECI \to RTN} \end{bmatrix}$$

B.4.2   LVLH reference frame.

B.4.2.1   Definition.

The Local Vertical-Local Horizontal frame (LVLH) may be understood as a different interpretation of the RTN frame. It basically differs from it in the naming and direction of the axis, namely:

$$LVLH \equiv \begin{cases} \text{Origin} & \equiv & \text{Chief SC COM} \\[2ex] \text{Z-axis}(-\underline{e}_R) & \equiv & \text{Radial direction (positive inwards)} \\[2ex] \text{Y-axis}(-\underline{e}_N) & \equiv & \text{Normal to the orbit plane (cross-track)} \\ & & \text{(negative with orbit momentum)} \\[2ex] \text{X-axis}(\underline{e}_T) & \equiv & \text{Perpendicular to the Y and Z axes (along-track)} \\ & & \text{forming a right-handed system ($\approx$ tangent to the trajectory)} \end{cases}$$

B.4.2.2   State vector transformation.

There are two main ways to obtain the ECI to LVLH frame transformation:

A) Using reference orbit's Keplerian OEs.

This method is the one we have used for the PQW and the RTN frame. It is as easy as performing yet another rotation from the RTN frame, being consistent with the angular velocity.

Rotation matrix from ECI.

The additional rotation from RTN to LVLH is:

$$
R_{RTN \to LVLH} = \begin{bmatrix} 0 & 1 & 0 \\ 0 & 0 & -1 \\ -1 & 0 & 0 \end{bmatrix}
$$

leading to the full rotation matrix:

$$
R_{ECI \to LVLH} = R_{ECI \to RTN} R_{RTN \to LVLH} = \begin{bmatrix} -C\Omega Su - S\Omega CiCu & C\Omega CiCu - S\Omega Su & CuSi \\ -S\Omega Si & C\Omega Si & -Ci \\ -C\Omega Cu + S\Omega CiSu & -C\Omega CiSu - S\Omega Cu & -SuSi \end{bmatrix}
$$

Angular velocity.

Although one could rotate either the vector or the matrix itself, it is actually easier to graphically derive the angular velocity (assuming of course unperturbed motion). Doing this, we can easily see that the only angular velocity component is the one in Y-axis, of value $-\dot{\theta}$. The angular velocity matrix then becomes:

$$
\Omega_{LVLH||ECI}|_{LVLH} = \begin{bmatrix} 0 & 0 & -\dot{\theta} \\ 0 & 0 & 0 \\ \dot{\theta} & 0 & 0 \end{bmatrix}
$$

B) Using reference ECI state vector.

This approach is based on [14], and was introduced in ??. For this transformation to be performed, we need to calculate the rotation matrix and its derivative. With this approach, that is analogous to get the unitary vectors expressed in ECI frame. As our inputs are actually the ECI coordinates and velocity of the chief spacecraft, this is almost already done. The unitary vectors of the rotating frame

in this case are:

$$
\begin{cases}
\underline{\hat{e}}_z = -\hat{\underline{r}} \\[2mm]
\underline{\hat{e}}_y = -\hat{\underline{h}} \\[2mm]
\underline{\hat{e}}_x = \underline{\hat{e}}_y \times \underline{\hat{e}}_z
\end{cases}
\tag{B.16}
$$

where $\hat{\underline{h}} = \dfrac{\underline{r} \times \underline{v}}{|\underline{r} \times \underline{v}|}$. $\underline{r}$ and $\underline{v}$ are respectively the position and velocity of the chief spacecraft.

Rotation matrix from ECI.

The rotation matrix $R_{ECI \to LVLH}$ is then:

$$
R_{ECI \to LVLH} = \begin{bmatrix} \underline{\hat{e}}_x{}^T \\[2mm] \underline{\hat{e}}_y{}^T \\[2mm] \underline{\hat{e}}_z{}^T \end{bmatrix}
$$

that is, each unitary vector is transposed into one row of the matrix.

Rotation matrix derivative.

By using equation (**??**) we can easily get the vectors' time derivatives:

$$
\begin{cases}
\dfrac{d}{dt}\left(\underline{\hat{e}}_z\right) & = & \dfrac{d}{dt}\left(-\hat{\underline{r}}\right) & = & -\dfrac{1}{r}\left[\underline{v} - (\hat{\underline{r}} \cdot \underline{v})\,\hat{\underline{r}}\right] \\[3mm]
\dfrac{d}{dt}\left(\underline{\hat{e}}_y\right) & = & \dfrac{d}{dt}\left(-\hat{\underline{h}}\right) & = & -\dfrac{1}{h}\left[\dot{\underline{h}} - \left(\hat{\underline{h}} \cdot \dot{\underline{h}}\right)\hat{\underline{h}}\right] \\[3mm]
\dfrac{d}{dt}\left(\underline{\hat{e}}_x\right) & = & \dfrac{d}{dt}\left(\underline{\hat{e}}_y \times \underline{\hat{e}}_z\right) & = & \dfrac{d}{dt}\left(\underline{\hat{e}}_y\right) \times \underline{\hat{e}}_z + \underline{\hat{e}}_y \times \dfrac{d}{dt}\left(\underline{\hat{e}}_z\right)
\end{cases}
$$

where all entities are known except for $\dot{\underline{h}}$, which is in turn:

$$
\dot{\underline{h}} = \dfrac{d}{dt}\left(\underline{r} \times \underline{v}\right) = \underline{r} \times \underline{a}
$$

Hence, the acceleration of the chief spacecraft needs to be provided when it is not radial. As that is the case with the unperturbed two-body problem, the rotation matrix is significantly simplified:

$$
\begin{cases}
\dfrac{d}{dt}\left(\underline{\hat{e}}_z\right) & = & -\dfrac{1}{r}\left[\underline{v} - (\hat{\underline{r}} \cdot \underline{v})\,\hat{\underline{r}}\right] \\[3mm]
\dfrac{d}{dt}\left(\underline{\hat{e}}_y\right) & = & \underline{0} \\[3mm]
\dfrac{d}{dt}\left(\underline{\hat{e}}_x\right) & = & -\hat{\underline{h}} \times \dfrac{d}{dt}\left(\underline{\hat{e}}_z\right)
\end{cases}
$$

The construction of $\dot{R}_{ECI \to LVLH}$ is identical to its primitive. The transformation matrices can now be built, following equations **??** and **??**.
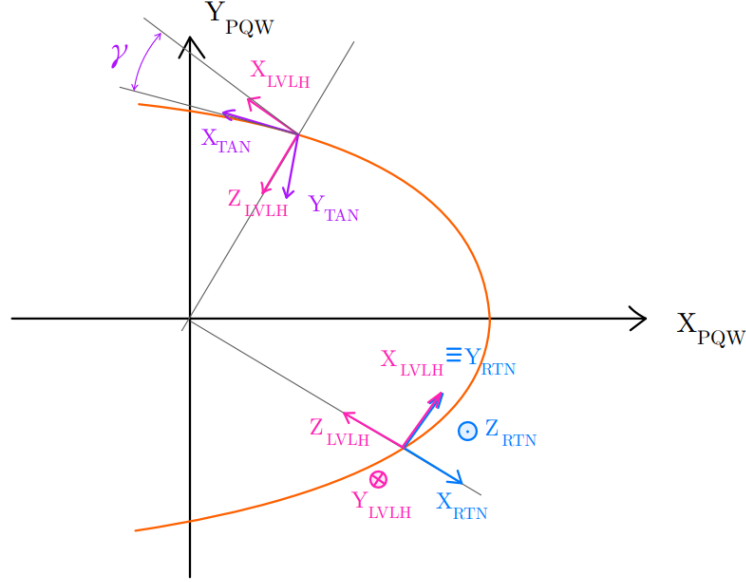
B.4.3   TAN reference frame.

Figure B.6: Relative reference frames.

B.4.3.1   Definition.

The Tangent reference frame (TAN) is quite similar to the LVLH frame, but instead of featuring an axis pointing towards *nadir* (Earth), this frame includes an axis pointing always in the velocity direction. This involves a simple rotation from the LVLH frame, of an angle γ called flight path angle (see figure **??**). It is then unsurprisingly defined as the angle between the horizon (local horizontal) and the velocity vector. Let us then analyze the transformation from the LVLH frame.

B.4.3.2   State vector transformation.

Rotation matrix from LVLH.

In this case, it is a simple clockwise rotation around LVLH Y-axis, that is:

$$R_{LVLH \to TAN} = \begin{bmatrix} \cos\gamma & 0 & -\sin\gamma \\ 0 & 1 & 0 \\ \sin\gamma & 0 & \cos\gamma \end{bmatrix}$$

Angular velocity.

As it has been explained before, let us just write the angular velocity matrix as:

$$\Omega_{LVLH \to TAN}|_{LVLH} = \begin{bmatrix} 0 & 0 & -\dot{\gamma} \\ 0 & 0 & 0 \\ \dot{\gamma} & 0 & 0 \end{bmatrix}$$

There is something remaining: γ and its derivative must be calculated. Starting with the angle itself, its sine and cosine satisfy:

$$\begin{cases} \sin\gamma &= \dfrac{e\sin\theta}{\Theta} \\ \cos\gamma &= \dfrac{\rho}{\Theta} \end{cases}$$

where $\Theta = \sqrt{2\rho - \eta^2}$. γ is simply calculated as:

$$\gamma = \text{atan2}\left(\sin\gamma,\ \cos\gamma\right)$$

On the other hand, $\dot{\gamma}$ can be calculated as:

$$\dot{\gamma} = n\frac{\rho^2\left(\rho - \eta^2\right)}{\eta^3\Theta^2}$$

Therefore, the transformation is complete.

B.5   Conversions from OEs to cartesian coordinates.

B.5.1   Keplerian OEs to ECI and vice versa.

B.5.1.1   KOE to ECI transformation.

Let us start with the simpler, unambiguous transformation. By considering the perifocal coordinates $(q, \dot{q})$ (see **??**), we can easily derive an explicit relation from Keplerian OEs to the ECI state vector:

$$\begin{cases} x &= (\cos\Omega\cos u - \sin\Omega\cos i\sin u) & r \\ y &= (\sin\Omega\cos u + \cos\Omega\cos i\sin u) & r \\ z &= (\sin i\sin u) & r \\ \dot{x} &= (\cos\Omega\cos u - \sin\Omega\cos i\sin u)\ v_R - (\cos\Omega\sin u + \sin\Omega\cos i\cos u)\ v_T \\ \dot{y} &= (\sin\Omega\cos u + \cos\Omega\cos i\sin u)\ v_R - (\sin\Omega\sin u - \cos\Omega\cos i\cos u)\ v_T \\ \dot{z} &= (\sin i\sin u) \hspace{3.5cm} v_R + (\cos u\sin i) \hspace{1cm} v_T \end{cases}$$

where v_R and v_T are the radial and tangential velocities, namely:

$$
\begin{cases}
v_R & = & \dot{r} & = & \dfrac{h}{p} e \sin\theta \\[2em]
v_T & = & r\dot{\theta} & = & \dfrac{h}{p}\rho
\end{cases}
$$

B.5.1.2   ECI to KOE transformation.

This transformation is considerably more complex. For that reason, the relations will not be entirely justified. These are the following:

- Semimajor axis: Directly from energy equation:

$$
a = \frac{r}{2 - \dfrac{rv^2}{\mu}}
$$

- Eccentricity: Prior relations arise from (a) the dot product of velocity and position and (b) the polar equation of the ellipse:

$$
\begin{cases}
e \sin\theta & = & \dfrac{h}{\mu r}\underline{r} \cdot \underline{v} \\[1.5em]
e \cos\theta & = & \dfrac{p}{r} - 1
\end{cases}
\quad\Rightarrow\quad e = \sqrt{(e\sin\theta)^2 + (e\cos\theta)^2}
$$

where p is the orbit parameter.

- Inclination From the orientation of the angular momentum vector:

$$
i = \text{atan2}\left(h_{xy},\ h_z\right)
$$

where $h_{xy} = \sqrt{h_x^2 + h_y^2}$

The remaining elements (Ω, ω and M) depend on the type of the orbit. As we know, if the orbit is equatorial ($i = 0$), Ω and ω are not defined by themselves. Furthermore, if the orbit is circular, not even ω is defined, and therefore we have to make some adjustments. In the first case, we will assume $\varpi = \omega + \Omega$ as our fifth element, and the fourth will be null. In the second case, we will merge all values into the mean anomaly, assuming both ω and Ω to be null.

Case A) Non-singular eccentricity or inclination.

$$
\begin{cases}
\Omega &=& \mathrm{atan2}\,(h_x,\,-h_y) \\
u &=& \mathrm{atan2}\,(h \cdot z,\,y \cdot h_x - x \cdot h_y) \\
\theta &=& \mathrm{atan2}\,(e \sin\theta,\,e \cos\theta) \\
\omega &=& u - \theta
\end{cases}
$$

Case B) Null inclination, non-singular eccentricity.

$$
\begin{cases}
\Omega &=& 0 \\
u &=& \mathrm{atan2}\,(y, x) \cdot \mathrm{sign}(h_z) \\
\theta &=& \mathrm{atan2}\,(e \sin\theta, e \cos\theta) \\
\omega &=& u - \theta
\end{cases}
$$

Case C) Null eccentricity, non-singular inclination.

Auxiliary definitions:

$$
\begin{cases}
\underline{N} &=& \hat{\underline{e}}_z \times \underline{h} \\
N_{xy} &=& \sqrt{N_x^2 + N_y^2} \\
S &=& \mathrm{sign}\,((\underline{e} \times \underline{r}) \cdot \underline{h})
\end{cases}
$$

Element computation:

$$
\begin{cases}
\Omega &=& \mathrm{atan2}\,(h_x, -h_y) \\
\omega &=& 0 \\
\theta &=& S \cdot \arccos\left(\dfrac{r}{r}, \dfrac{\underline{N}}{N_{xy}}\right)
\end{cases}
$$

Case D) Null eccentricity and inclination.

$$
\begin{cases}
\Omega &=& 0 \\
\omega &=& 0 \\
\theta &=& \mathrm{atan2}(y, x) \cdot \mathrm{sign}(h_z)
\end{cases}
$$

B.5.2 Relative Keplerian OEs to RTN.

Although one can technically go from RKOEs to RTN coordinates in several steps already described, there is a direct mapping between them, developed by H. Schaub [11]. Without further

ado, the position mapping is expressed as follows:

$$
\begin{cases}
x \approx \dfrac{r}{a}\delta a + \dfrac{ae\sin\theta}{\eta}\delta M - a\,\cos\theta\delta e & \text{(B.17a)} \\[2ex]
y \approx \dfrac{r\rho^2}{\eta^3}\delta M + r\delta\omega + \dfrac{r\sin\theta}{\eta^2}(\rho+1)\delta e + r\cos i\delta\Omega & \text{(B.17b)} \\[2ex]
z \approx r\left(\sin u\delta i - \cos u\sin i\delta\Omega\right) & \text{(B.17c)}
\end{cases}
$$

Nonetheless, the mapping for the velocity is expressed in terms of relative quasi-non-singular OEs [17]. For the conversion from RKOEs to these, please see **??**:

$$
\begin{cases}
\dot{x} \approx & -\dfrac{V_r}{2a}\delta a + \left(\dfrac{1}{r}-\dfrac{1}{p}\right)h\delta u & \text{(B.18a)} \\[2ex]
& + (V_r a q_1 + h\sin u)\dfrac{\delta q_1}{p} + (V_r a q_2 - h\cos u)\dfrac{\delta q_2}{p} & \text{(B.18b)} \\[2ex]
\dot{y} \approx & -\dfrac{3V_t}{2a}\delta a - V_r\delta u + (3V_t a q_1 + 2h\cos u)\dfrac{\delta q_1}{p} & \text{(B.18c)} \\[2ex]
& + (3V_t a q_2 + 2h\sin u)\dfrac{\delta q_2}{p} + V_r\cos i\delta\Omega & \text{(B.18d)} \\[2ex]
\dot{z} \approx & (V_t\cos u + V_r\sin u)\,\delta i & \text{(B.18e)} \\[2ex]
& + (V_t\sin u - V_r\cos u)\sin i\delta\Omega & \text{(B.18f)}
\end{cases}
$$

The mapping represented by equations (**??**) and (**??**) is a linear approximation, in which it is assumed that the relative distance between spacecrafts is much smaller than the chief's orbital radius. For more in-depth content about this transformation, please see [11, 17].

Bibliography

General

Books

[6] W. E. Wiesel. Modern Astrodynamics. 2nd ed. Beavercreek, Ohio: Aphelion Press, 2010.

[13] P. K. S. Dennis D. McCarthy. Time: From Earth Rotation to Atomic Physics. Wiley-VCH, 2009. isbn: 3527407804; 9783527407804.

[15] B. D. Tapley, B. E. Schutz, and G. H. Born. Statistical Orbit Determination. 1st ed. Amsterdam, Netherlands: Elsevier, 2004.

[18] O. Montenbruck and E. Gill. Satellite Orbits: Models, Methods and Applications. 1st ed. Wessling, Germany: Springer, 2001.

[19] K. T. Alfriend and Srinivas. Spacecraft Formation Flying. 1st ed. Oxford, United Kingdom: Elsevier, 2010.

[20] R. H. Battin. An Introduction to the Mathematics and Methods of Astrodynamics, Revised Edition. 1st ed. Reston, Virginia: American Institute of Aeronautics and Astronautics, 1999 (cit. on p. 5).

[21] D. Brouwer and G. M-Clemence. Methods of Celestial Mechanics. Brackley Square House, London: Academic Press, 1961.

[22] H. Schaub and J. L. Junkins. Analytical Mechanics of Space Systems. Reston, VA: AIAA Education Series, Oct. 2003. doi: 10.2514/4.861550.

Articles

[1] J. Sullivan, S. Grimberg, and S. D'Amico. Comprehensive Survey and Assessment of Spacecraft Relative Motion Dynamics Models. In: *Journal of Guidance, Control & Dynamics* 40.8 (2017), pp. 1837–1859. doi: 10.2514/1.G002309.

[11] H. Schaub. Relative Orbit Geometry Through Classical Orbit Element Differences. In: *Journal of Guidance, Control & Dynamics* 27.5 (2004), pp. 839–848. doi: 10.2514/1.12595.

[17] H. Schaub and K. T. Alfriedn. Hybrid Cartesian and Orbit Element Feedback Law for Formation Flying Spacecraft. In: *Journal of Guidance, Control & Dynamics* 25.2 (2002), pp. 387–393. DOI: 10.2514/2.4893.

[25] N. Capitaine. The Celestial Pole Coordinates. In: *Celestial Mechanics and Dynamical Astronomy* 48 (1990), pp. 127–143.

Eccentric Dynamics

Articles

[2] J. Tschauner and P. Hempel. Optimale Beschleunigungsprogramme für das Rendezvous-Manöver. In: *Astronautica Acta* 10 (1964), pp. 296–307.

[4] K. Yamanaka and F. Ankersen. New State Transition Matrix for Relative Motion on an Arbitrary Elliptical Orbit. In: *Journal of Guidance, Control & Dynamics* 25.1 (2002), pp. 60–66. DOI: 10.2514/2.4875 (cit. on p. 1).

[5] T. Vincent Peters and R. Noomen. Linear Cotangential Transfers and Safe Orbits for Elliptic Orbit Rendezvous. In: *Journal of Guidance, Control & Dynamics* 44.4 (2021), pp. 732–748. DOI: 10.2514/1.G005152.

[7] M. Eckstein, C. Rajasingh, and P. Blumer. Colocation Strategy and Collision Avoidance for the Geostationary Satellites at 19 Degrees West. In: *CNES International Symposium on Space Dynamics*. Vol. 25. Oberpfaffenhofen, Germany: DLR GSOC, Nov. 1989, pp. 60–66 (cit. on p. 4).

[8] S. D'Amico and O. Montenbruck. Proximity Operations of Formation-Flying Spacecraft Using an Eccentricity/Inclination Vector Separation. In: *Journal of Guidance, Control & Dynamics* 29.3 (2006), pp. 554–563. DOI: 10.2514/1.15114.

[26] R. Broucke. On the Matrizant of the Two-Body Problem. In: *Astronomy and Astrophysics* 6 (June 1970), p. 173.

Perturbations

Books

[23] A. H. Nayfeh. Perturbation Methods. Weinheim, Germany: Wiley-VCH, 2004.

[24] W. M. Kaula. Theory of Satellite Geodesy. Mineola, New York: Dover Publications, 2013.

Articles

[9]   D.-W. Gim and K. T. Alfriend. Satellite Relative Motion Using Differential Equinoctial Elements. In: *Celestial Mechanics and Dynamical Astronomy* 92.4 (2005), pp. 295–336. DOI: 10.1007/s10569-004-1799-0.

[10] S. D'Amico. Relative Orbital Elements as Integration Constants of Hill's Equations. TN 05-08. Deutsches Zentrum für Luft- und Raumfahrt (DLR), 2005.

[12] G. Gaias, C. Colombo, and M. Lara. Accurate Osculating/Mean Orbital Elements Conversions for Spaceborne Formation Flying. In: (Feb. 2018). https://www.researchgate.net/publication/340378956_Accurate_OsculatingMean_Orbital_Elements_Conversions_for_Spaceborne_Formation_Flying.

[27] D.-W. Gim and K. Alfriend. State Transition Matrix of Relative Motion for the Perturbed Noncircular Reference Orbit. In: *Journal of Guidance Control and Dynamics* 26 (Nov. 2003), pp. 956–971. DOI: 10.2514/2.6924.

[28] G. Gaias, J.-S. Ardaens, and C. Colombo. Precise line-of-sight modelling for angles-only relative navigation. In: *Advances in Space Research* 67.11 (2021). Satellite Constellations and Formation Flying, pp. 3515–3526. DOI: 10.1016/j.asr.2020.05.048.

[29] G. Gaias, C. Colombo, and M. Lara. Analytical Framework for Precise Relative Motion in Low Earth Orbits. In: *Journal of Guidance, Control, and Dynamics* 43.5 (2020), pp. 915–927. DOI: 10.2514/1.G004716.

[30] D. Brouwer. Solution of the problem of artificial satellite theory without drag. In: *Astronomical Journal* 64.5 (Nov. 1959), p. 378. DOI: 10.1086/107958.

[31] R. H. Lyddane. Small eccentricities or inclinations in the Brouwer theory of the artificial satellite. In: *Astronomical Journal* 68 (Oct. 1963), p. 555. DOI: 10.1086/109179.

Matlab Exchange libraries

[34] F. G. Nievinski. subtightplot. https://www.mathworks.com/matlabcentral/fileexchange/39664-subtightplot. 2013.

[35] J. C. Lansey. linspecer. https://www.mathworks.com/matlabcentral/fileexchange/42673-beautiful-and-distinguishable-line-colors-colormap. 2015.

[36] Jan. WindowAPI. https://www.mathworks.com/matlabcentral/fileexchange/31437-windowapi. 2013.

[37]   T. Davis. Arrow3. https://www.mathworks.com/matlabcentral/fileexchange/14056-arrow3. 2022.